AD-A185 899 INTERFACE EFFECTS ON THE MECHANICAL PROPERTIES OF CERAMIC COMPOSITES(U) ROCKWELL INTERNATIONAL THOUSAND OAKS CA SCIENCE CENTER D B MARSHALL SEP 87 SC5432.AR 1/1

UNCLASSIFIED N00014-85-C-0416 F/G 11/2 NL

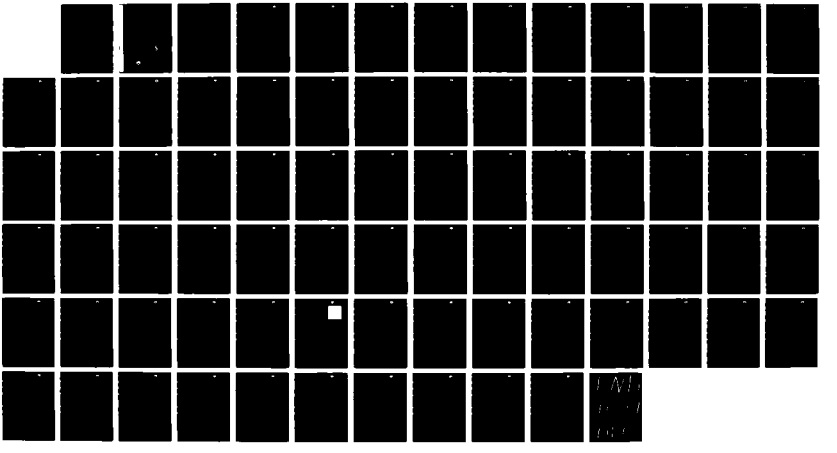

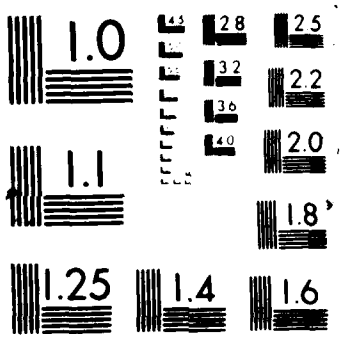
1.0
1.1
1.25
1.4
1.6
1.8
2.0
2.2
2.5
2.8
3.2
3.6
4.0

(11)

Copy No. 4

SC5432.AR

INTERFACE EFFECTS ON THE MECHANICAL PROPERTIES OF CERAMIC COMPOSITES

ANNUAL REPORT NO. 2 FOR THE PERIOD
July 15, 1986 through July 14, 1987

CONTRACT NO. N00014-85-C-0416

Prepared for

Scientific Officer
Program Manager Nonmetallic Materials
Office of Naval Research
800 N. Quincy Street
Arlington, VA 22217-5000

D.B. Marshall
Principal Investigator

SEPTEMBER 1987

Rockwell International
Science Center

UNCLASSIFIED

SECURITY CLASSIFICATION OF THIS PAGE

ADA185899

REPORT DOCUMENTATION PAGE

1a REPORT SECURITY CLASSIFICATION **UNCLASSIFIED**	1b. RESTRICTIVE MARKINGS
2a SECURITY CLASSIFICATION AUTHORITY	3. DISTRIBUTION/AVAILABILITY OF REPORT **Approved for public release; distribution unlimited**
2b CLASSIFICATION/DOWNGRADING SCHEDULE	
4 PERFORMING ORGANIZATION REPORT NUMBER(S) **SC5432.AR**	5. MONITORING ORGANIZATION REPORT NUMBER(S)
6a NAME OF PERFORMING ORGANIZATION **ROCKWELL INTERNATIONAL Science Center** 6b OFFICE SYMBOL *(If Applicable)*	7a NAME OF MONITORING ORGANIZATION
6c ADDRESS *(City, State, and ZIP Code)* **1049 Camino Dos Rios Thousand Oaks, CA 91360**	7b. ADDRESS *(City, State and ZIP Code)*
8a NAME OF FUNDING/SPONSORING ORGANIZATION **Scientific Officer, Program Manager Nonmetallic Materials** 8b OFFICE SYMBOL *(If Applicable)*	9. PROCUREMENT INSTRUMENT IDENTIFICATION NUMBER **CONTRACT NO. NOOO14-85-C-0416**
8c ADDRESS *(City, State and ZIP Code)* **Office of Naval Research 800 N. Quincy Arlington, VA 22217**	10. SOURCE OF FUNDING NOS. PROGRAM ELEMENT NO. / PROJECT NO. / TASK NO / WORK UNIT NO
11 TITLE *(Include Security Classification)* **INTERFACE EFFECTS ON THE MECHANICAL PROPERTIES OF CERAMIC COMPOSITES**	
12 PERSONAL AUTHOR(S) **Marshall, D.B.**	
13a TYPE OF REPORT **Annual Report No. 2**	13b TIME COVERED FROM **07/15/86** TO **07/14/87**
14 DATE OF REPORT *(Yr., Mo., Day)* **1987, SEPTEMBER**	15 PAGE COUNT **78**
16 SUPPLEMENTARY NOTATION	

17 COSATI CODES		
FIELD	GROUP	SUB GR.

18 SUBJECT TERMS *(Continue on reverse if necessary and identify by block number)*

19. ABSTRACT *(Continue on reverse if necessary and identify by block number)*

Macroscopic and microscopic mechanical properties of ceramic composites have been investigated. A fracture mechanics analysis was developed to evaluate the influence of residual microstructural stresses on the fracture toughness of composites that are reinforced by crack bridging mechanisms. The magnitude and sign of the toughening were found to be very sensitive to the details of the bridging mechanism and the criterion for ligament rupture. These results highlight the need for techniques to measure microscopic mechanical properties such as residual stresses, interfacial debonding and sliding resistance, and deformation and fracture of small reinforcements. Further analysis of an indentation fiber-pushing technique that was developed previously under this contract for measuring fiber-matrix interfacial properties has enabled the technique to be used to measure residual stresses in individual fibers and to measure frictional sliding resistance in carbon fiber composites.

20 DISTRIBUTION/AVAILABILITY OF ABSTRACT UNCLASSIFIED/UNLIMITED ☐ SAME AS RPT ☒ DTIC USERS ☐	21. ABSTRACT SECURITY CLASSIFICATION **UNCLASSIFIED**
22a NAME OF RESPONSIBLE INDIVIDUAL	22b. TELEPHONE NUMBER *(Include Area Code)* / 22c OFFICE SYMBOL

DD FORM 1473, 83 APR EDITION OF 1 JAN 73 IS OBSOLETE

UNCLASSIFIED

SECURITY CLASSIFICATION OF THIS PAGE

TABLE OF CONTENTS

1.0 INTRODUCTION

The goal of this research is to develop a basic scientific understanding of the relation between the macroscopic mechanical properties of ceramic composites and the properties of the microstructure, especially the fiber-matrix interface. The work is directed to two main topics. One is to devise experiments that are capable of measuring the properties of the fiber-matrix interface directly, and the other is to develop micro-mechanics models that relate the interface properties quantitatively to the strength, toughness and failure mechanisms of the composite.

Detailed results of research done during the past year are contained in four papers which are included as Sections 2.0 to 5.0 of this report, and which have been submitted to, or published, in the journals and books noted on the title pages. The results from these sections and from other work that is under way are briefly summarized below.

The fracture mechanics modeling addressed the problem of evaluating the influence of residual microstructural stresses on the fracture toughness of ceramics and ceramic composites that are reinforced by crack bridging mechanisms (Sections 2.0 and 3.0). The residual stresses were shown to influence the toughness by modifying the stress-displacement relation for stretching of the crack bridging ligaments. This simple result is rigorously correct, but not at all obvious. Modified toughnesses were calculated using a J-integral analysis for several typical stress-displacement laws. The magnitude and sign of the toughening were found to be strongly dependent upon the details of the bridging mechanism and the criterion for ligament rupture. These results highlight the need for a thorough understanding of the mechanics of the ligament separation process, as well as the need for techniques to measure microscopic mechanical properties, such as interfacial debonding and sliding resistance, deformation of small constrained volumes, and fracture properties of small reinforcements. The analysis was also used to derive the condition for spontaneous matrix cracking due to residual tensile stress in the matrix.

In the previous year of this contract, a fracture mechanics model was developed to predict failure mechanisms, failure stresses and fracture toughnesses of composites with aligned, frictionally bonded reinforcements. Two analyses are under way to extend this model. One involves derivation of a stress-displacement relation for reinforcements that undergo limited slip (previously the extremes of no slip and large slip

had been analyzed) and obtaining numerical solutions from the fracture mechanics model for the matrix cracking stress. The other analysis involves the effect of statistical variations in the strengths of the reinforcing fibers (previously a deterministic fiber strength was taken). Results of these analysis which have been partly completed will be submitted for publication within the next two months.

In the studies of fiber-matrix interface properties, novel methods were developed during the previous year of this contract for investigating bonding at the interface and to measure sliding resistance. These are based on an indentation technique in which the ends of individual fibers are pushed with a diamond indenter, and the forces and displacements are measured continuously during loading, unloading and load cycling. During the current year, analysis of the fiber sliding process has been extended to evaluate the influence of microstructural residual stress, and thereby allow measurement of the residual stresses from the modified force-displacement relations (Section 3.0). Preliminary experiments using SiC/glass ceramic composites have shown that residual stresses are generated by thermal cycling in an inert environment. The influence of these residual stresses on mechanical reliability of the composite will be assessed.

The range of composites to which the indentation method can be applied has been extended by recognizing that load-displacement measurements during load cycling can be used directly, without calibration of the indenter penetration into the fiber, to evaluate frictional stresses. Previously, calibration of the indenter penetration was needed to calculate the relative sliding of the fiber and matrix. This was obtained in the SiC/glass-ceramic system either from measurements of residual hardness impressions in the fibers or by calibration tests on composites that were heat treated to create a strongly bonded interface that did not undergo sliding. However, neither of these calibration methods could be applied to carbon fiber-reinforced glass and glass-ceramic composites, because the interfaces in these systems could not be easily bonded and the combination of small fiber radius and low frictional resistance was such that the indenter contact with the fiber was purely elastic. Moreover, the accuracy of calculation of the elastic penetration was limited by uncertainties in the indenter profile and anisotropic elastic properties of the fiber. These problems were circumvented by using the displacement measurements during unloading and reloading, along with appropriate analysis of fiber sliding, to evaluate the frictional stress.

Finally, calculations are in progress to evaluate the role of Poisson's expansion and contraction of the fibers during fracture and fiber pushing experiments. In our previous indentation analyses, this effect was neglected and independent experimental measurements confirmed the validity of this approximation in the SiC/glass-ceramic composites. However, because of the widespread interest that the technique has generated in the composites community, it is important to define the range of material and interfacial properties for which the approximation is valid and to provide analysis that can be used for those composites in which it is not valid.

2.0 THE INFLUENCE OF RESIDUAL STRESS ON THE TOUGHNESS OF REINFORCED BRITTLE MATERIALS

Materials Forum, in press

THE INFLUENCE OF RESIDUAL STRESS ON THE TOUGHNESS OF REINFORCED BRITTLE MATERIALS

D.B. Marshall

Rockwell International Science Center
1049 Camino Dos Rios
Thousand Oaks, CA 91360

and

A.G. Evans

Department of Materials
University of California
Santa Barbara, CA 93106

ABSTRACT

Residual microstructural stresses in ceramics and ceramic composites are shown to influence the fracture toughness by modifying the stress-displacement relation for stretching of crack-bridging ligaments. Modified toughnesses are calculated using a J-integral analysis for several typical stress-displacement laws. The magnitude and sign of the toughening are found to be strongly dependent upon the details of the bridging mechanism and the criterion for ligament rupture. The analysis is also used to derive the condition for spontaneous matrix cracking due to residual tensile stress in the matrix.

1.0 INTRODUCTION

Many brittle matrix composites[1-11] and single-phase polycrystalline ceramics[12-15] have toughnesses strongly influenced by the presence of intact ligaments between the crack surfaces. The degree of toughening is dictated by the stress-displacement law governing the extension of the bridging ligaments and their eventual rupture.[16] For materials reinforced with ductile dispersions, reinforcement rupture is essentially displacement controlled. Conversely, for materials reinforced by brittle ligaments (fibers, whiskers, particles or interlocking grains), the reinforcement rupture may be either stress controlled or displacement controlled, depending on whether ligament fracture or pullout is dominant. It will be demonstrated in this paper that the existence of microstructural residual stresses in such materials can strongly influence the fracture toughness, and that this influence can be profoundly dependent upon both the functional form of the stress-displacement law and whether the reinforcement rupture is stress or displacement controlled.

Residual microstructural stresses arise generally from thermal contraction during cooling from an elevated processing temperature. The residual stresses before cracking are of opposite sign in the reinforcing ligaments and matrix, and the average residual stress normal to a potential crack plane that spans many microstructural units is zero. Therefore, in the absence of a bridging zone, the microstructural residual stresses have no effect on the steady-state fracture toughness. However, when a bridging zone exists, residual stresses influence the fracture toughness, through their effect on the stress-displacement law for ligament stretching.

2.0 ANALYSIS OF TOUGHENING

2.1 Toughening from Bridging Ligaments

The influence of crack bridging ligaments on the steady-state fracture toughness may be analyzed conveniently by making use of the J-integral,[19] as previously applied to bridging problems by Rose[20] and Budiansky.[16] For the closed path shown in Fig. 1, there are three contributions to the J-integral:

$$J_\infty - J_B - J_{tip} = 0 \ . \tag{1}$$

The term J_B from the path over the bridged crack surface represents the increase in fracture energy due to the ligaments, and is given by

$$J_B = 2 \int_0^{u^*} \sigma\,(u)du \tag{2}$$

where $\sigma(u)/f$ is the stress exerted by a ligament at an average matrix crack opening u, with u* being the crack opening above which the ligaments cease to restrain the crack surfaces, and f is the fraction of the crack area covered by ligaments. The contribution from the outer path is

$$J_\infty = K_\infty^2(1 - \nu^2)/E \ , \tag{3}$$

where K_∞ is the remotely applied stress intensity factor and E is the Young's modulus. Then, if we set $J_{tip} = J_o$ (i.e., the critical value of J for crack extension in the absence of bridging forces) Eq. (1), defines a condition for crack growth:

$$K_a^2(1 - \nu^2)/E = 2\int_o^{u^*} \sigma(u)du + J_o \ . \tag{4}$$

Equation (4) can be expressed in terms of the critical stress intensity factor K_o defined by

$$K_o = \sqrt{EJ_o/(1-\nu^2)} \ , \tag{5}$$

and the fracture toughness increase,

$$K_B = K_a - K_o \ , \tag{6}$$

to give

$$K_B/K_o = \left[1 + \frac{2E}{(1-\nu^2)K_o^2}\int_o^{u^*} \sigma(u)\, du\right]^{1/2} - 1 \ . \tag{7}$$

The toughness increase can be derived alternatively by calculating the reduction in stress intensity factor due to the stresses exerted on the crack surfaces by the bridging ligaments;[21]

$$K_B = 2\sqrt{\frac{c}{\pi}} \int_{c-L}^{c} \frac{\sigma(x)dx}{\sqrt{c^2 - x^2}}, \tag{8}$$

where c is the crack length, L is the length of the bridging zone, and x is the distance from the crack mouth. Equations (7) and (8) must provide equivalent solutions for the toughness increase. This has been demonstrated for a bridging zone with uniform tractions[22] (i.e., a Dugdale zone). Equivalence is also readily demonstrated for nonuniform stresses in the limit $K_B/K_o \to 0$, whereupon the crack opening is defined by the near tip profile (i.e., $u = \sqrt{8/\pi}\ K_o \sqrt{c - x}/E$) and both Eqs. (7) and (8) reduce to

$$K_B = \frac{E}{K_o} \int_o^{u^*} \sigma(u)\ du \tag{9}$$

However, in general, calculations of $\sigma(x)$ in Eq. (8) and the upper limit of integration, u^*, in Eq. (7) require solution of an integral equation for the crack opening, $u(x)$. For the special case of the steady-state toughening, where u^* is a fixed value defined by the ligament rupture condition, solution for $u(x)$ is not necessary and K_B is more readily evaluated from the J-integral approach (Eq. (7)).

3.0 ROLE OF RESIDUAL STRESSES

3.1 Stress-Displacement Law

The above results are unaltered in form by the presence of microstructural residual stresses. However, the residual stresses influence the fracture toughness through their influence on the bridging stresses $\sigma(u)$ in Eq. (7) and $\sigma(x)$ in Eq. (8) (as well as the limit of integration, defined by the bridging zone length, L).

The bridging stresses $\sigma(u)$ are defined by the stress-displacement relation for an element between x and x + dx within the bridged zone, as shown in Fig. 2(a). Representative functions in the absence of residual stresses are illustrated in Fig. 2(b) for elastic, frictionally bonded, and ductile reinforcements. Brittle ligaments that fail between the crack surfaces are characterized by monotonically increasing $\sigma(u)$ functions, whereas, failure of the reinforcement within the matrix can lead to extensive pullout with decreasing $\sigma(u)$. The response of ductile reinforcements is sensitive to whether or not they are fully bonded to the matrix; deformation of bonded reinforcements is constrained by the matrix, resulting in a peak stress that is much higher than the uniaxial yield stress.[22]

To illustrate the influence of residual stresses on the bridging forces, consider a composite with unidirectionally aligned reinforcing fibers. If the average residual stress parallel to the fibers in the

uncracked matrix is σ_m^R, then equilibrium requires that the residual stress in the fibers be (Fig. 3(a))

$$\sigma_f^R = -\sigma_m^R(1 - f)/f \ . \tag{10}$$

This residual stress causes an offset in the origin of the $\sigma(u)$ function, which may be evaluated by imagining applying stress σ_o to the composite to cancel the stress in the matrix, and then cutting the matrix (across the plane AA' in Fig. 3(b)) to form a crack without causing displacement of the crack surfaces (i.e., $u = 0$). The requisite applied stress is

$$\sigma_o = -\sigma_m^R \, E/E_m \tag{11}$$

where E_m and E_f are the Young's moduli of the matrix and fibers. The resultant stress in the fibers is σ_o/f.

Upon subsequent application of stress, the initial crack opening displacements can be estimated by simply translating the $\sigma(u)$ curve along the stress axis (Fig. 4), i.e.

$$\sigma(u) - \sigma_o = \sigma^o(u) \tag{12}$$

where $\sigma(u)$ is the net applied stress and $\sigma^o(u)$ is the stress-displacement relation in the absence of residual stress. For <u>linear elastic</u> ligaments, this result follows directly from stress superposition. For constrained

(bonded) ductile reinforcements, finite element analysis[23] has established that the initial deformation is not significantly influenced by hydrostatic residual stress in the particles. Equation (13) also holds for frictionally bonded reinforcements (Appendix A) if the frictional forces arise solely from surface roughness. However, for frictional forces following a Coulomb law, the function $\sigma^o(u)$ in Eq. (13) contains a proportionality constant that is dependent on the magnitude of σ_R. The ultimate stress and the decreasing portions of the $\sigma(u)$ curves are of course sensitive to the details of the individual bridging mechanisms. Generally, however, for brittle reinforcements, either stress or displacement controlled failure criteria can be envisioned,[17,18,24] whereas, for ductile reinforcements displacement controlled failure is expected.

3.2 Influence of Residual Stresses on Toughening

The role of residual stresses can be conveniently illustrated by considering a linear spring model with a stress-displacement function

$$\sigma^o(u) = \begin{cases} \alpha u & u < u_c \\ o & u > u_c \end{cases} \qquad (13)$$

The modified $\sigma(u)$ functions in the presence of compressive and tensile residual stresses are shown in Fig. 5, along with the corresponding distributions of tractions on the crack surfaces within the bridging zone. For com-

pressive residual stress in the matrix ($\sigma_o > 0$, Eq. (11)), the stresses in the ligaments are always tensile and the ligaments exert closure forces on the crack. However, if the residual stress in the matrix is tensile ($\sigma_o < 0$), the ligaments experience compressive stresses for crack openings smaller than u_o. Therefore, the ligaments exert opening forces on the crack surfaces in the near-tip region where $u < u_o$, and closure forces further from the tip where $u > u_o$. The opening stresses contribute negtively to the toughening, as represented by the shaded (negative) area in Fig. 5(b).

The toughening increment in the absence of residual stress is (Eqs. (2) and (13)

$$J_B^o = \alpha u_c^2 \ . \tag{14}$$

In a residually stressed composite, the stress displacement function is

$$\sigma(u) = \begin{cases} \alpha u + \sigma_o & u < u^* \\ o & u > u^* \end{cases} \tag{15}$$

and the toughening increment is

$$J_B = 2u^*\sigma_o + \alpha u^{*2} \ . \tag{16}$$

The relative values of J_B and J_o are dependent upon the ligament failure criterion. If ligament rupture occurs at a critical stress, S, then $\sigma^o(u_c) \equiv \sigma(u^*) = Sf$ and

$$J_B/J_B^o = (1 + \Sigma)\ (1 - \Sigma)^{1/2} \tag{17}$$

where $\Sigma = \sigma^o/Sf = -\sigma_m^R\ E/E_m Sf$. On the other hand, if ligament failure is governed by a critical crack opening (i.e., $u^* = u_c = Sf/\alpha$), then

$$J_B/J_B^o = 1 + 2\Sigma \tag{18}$$

The variations of relative toughening with the residual stress parameter Σ are plotted in Fig. 6. Residual stresses always reduce the toughening when the matrix is in residual tension, but can either increase or decrease the toughening when the matrix is in compression, depending on the ligament failure condition; enhanced toughening results from displacement-controlled ligament rupture.

Analysis of more complex, nonlinear ligament response caused by interfacial sliding, debonding or plastic stretching (Appendix B) reveals that the influence of residual stress is very sensitive (in sign and magnitude) to the stress-displacement law as well as the ligament rupture criterion. The results of these analyses are summarized in Table 1.

4.0 SPONTANEOUS MATRIX CRACKING

Spontaneous cracking can occur in the matrix of a reinforced material if tensile residual stress in the matrix exceeds a critical value. The critical residual stress can be conveniently calculated using the analysis of Sect. 3. A compressive stress is first applied remotely to the composite in order to cancel the residual stress in the matrix, a slit is made in the matrix over the prospective crack plane, leaving the reinforcements intact, and the applied stress is then relaxed. Provided that the crack is sufficiently large, complete relaxation occurs in the ligaments remote from the crack tip and the crack opening approaches a limiting value u_o (Fig. 7). Closer to the crack tip the relaxation is constrained and compressive stresses remain in the bridging ligaments, which therefore exert opening forces on the crack surfaces (Fig. 7(b) and (c)). Since the bridging ligaments are stress-free beyond a certain distance, L_o, from the crack tip, the analysis of Sect. 3 can be applied directly. Thus, with $J_\infty = K_\infty^2(1 - \nu^2)/E = 0$, Eq. (4) provides a condition for spontaneous crack extension:

$$J_o + 2\int_0^{u_o} \sigma(u)\, du = 0 \,. \tag{19}$$

The integral in Eq. (19) is the shaded area (negative) beneath the stress-displacement curve, as shown in Fig. 7(c).

For reinforcements with a linear stress-displacement relation (Eq. (15)), evaluation of the integral in Eq. (19) (and substitution from Eq. (11)) gives a relation for the critical residual stress

$$\sigma_c^R = (\alpha J_o)^{1/2} E_m/E. \tag{20}$$

Similarly, for frictionally bonded reinforcements with the $\sigma(u)$ relation

$$\sigma(u) = \beta u^{1/2} + \sigma_o \tag{21}$$

the critical residual stress is

$$\sigma_c^R = [3J_o\beta^2/2]^{1/3} E_m/E. \tag{22}$$

These results for linear and frictionally bonded ligaments may be compared with previous, independent calculations by Budiansky et al,[25] who used a modified shear-lag analysis to calculate the strains in the fibers and matrix and, hence, the change in potential energy (strain energy, work done by loading system, and frictional work) associated with crack extension. From their analysis of strains in the fibers and matrix, the parameter α in the stress-displacement relation for linear ligaments has been evaluated[26] as

$$\alpha = \rho f E_f/R, \tag{23}$$

where ρ is a dimensionless constant involving ratios of elastic moduli of the fibers and matrix and the volume fraction of fibers. For frictionally bonded fibers, the corresponding result is given in Appendix A. Then, in terms of the fracture energy defined by Budiansky et al, $G_m = J_o/(1 - f)$, the condition for spontaneous cracking becomes

$$\sigma_R = \frac{E_m}{E}\left[\frac{f(1 - f)\rho E_f G_m}{R(1 - \nu^2)}\right]^{1/2} \tag{24}$$

for linear ligaments, and

$$\sigma_R = \frac{E_m}{E}\left[\frac{6f^2 E_f E \tau G_m}{(1 - \nu^2)E_m R}\right]^{1/3} \tag{25}$$

for frictionally bonded ligaments. These results are identical to those derived by Budiansky et al.[25]

5.0 DISCUSSION

The J-integral method for assessing the influence of microstructural residual stress on the steady-state toughness reduces to the problem of determining the modified stress-displacement relation for the bridging ligaments. The steady-state solution, which involves an integral (Eq. (4)) over the

entire stress-displacement curve, does not require explicit evaluation of crack opening displacements or bridging zone length. However, for a crack with a bridging zone smaller than the steady-state length, L, the upper limit of integration is $u < u^*$, and its evaluation requires solution of an integral equation for the crack opening displacements. Toughening is then characterized by a resistance curve and both the stress intensity and the J-integral approaches (Eqs. (7) and (8)) involve similar degrees of complexity.

The result illustrated in Fig. 5 has an interesting implication for the shape of the resistance curve in a composite with residual tension in the matrix. Since the bridging ligaments closest to the crack tip exert opening pressure on the crack surfaces, a crack that initially has no bridging zone (e.g., a crack emanating from a saw cut) experiences net opening forces from the developing bridging zone during the first stages of growth. Accordingly, the resistance curve must decrease initially, as illustrated in Fig. 8, and then increase under the influence of closure pressure that develops after further crack extension. The magnitude of the decrease in fracture energy at the minimum, ΔJ_o, increases with increasing residual stress. Furthermore, it may be noted that the condition for spontaneous cracking (Sect. 4) corresponds to the minimum occuring at $J = 0$.

Whether a residual stress causes an increase or decrease of the fracture energy is dependent on the details of the separation function and the ligament failure criterion. Results have been derived for several types of reinforcing ligaments (Table 1); brittle reinforcements characterized by linear springs (Sect. 3.2) or frictional restraint (Appendix B) and ductile

reinforcements strongly bonded to the matrix (Appendix B). Compressive residual stress in the matrix is found to enhance the toughening caused by bonded ductile reinforcements and by brittle reinforcements that are subject to displacement-controlled rupture and are either bonded (linear) or held in place by surface roughness. On the other hand, tensile residual stresses in the matrix are beneficial for the unbonded brittle reinforcement if the ligament rupture is dictated by a critical stress at the crack plane. Tensile residual stresses also enhance toughening if frictional restraining forces follow a Coulomb law and the extent of pullout is dictated by the length of a discontinuous reinforcement. However, in this case, the steady-state toughness may never be realized in practice, for the requisite crack opening displacement u^* is necessarily large (u^* is the length of the reinforcement rather than a plastic or elastic strain).

CONCLUSIONS AND IMPLICATIONS

Brittle matrix composites that have intact bridging reinforcements exhibit a toughness that can be strongly influenced by the residual stress. For ductile phase reinforced materials, the composite toughness is enhanced by having large residual tensile stresses in the reinforcement. Indeed, such large tensile stresses exist in many metal reinforced ceramic composites and may contribute importantly to the composite toughness. Microstructural modifications that enhance the residual stress are thus desirable and provide a rationale for toughness optimization. Composites reinforced with brittle

fibers/whiskers are subject to very different trends which are dependent upon specific details of the ligament separation process. For certain materials, residual tension in the matrix enhances the toughness because the seemingly negative role of residual tension can be offset by several mechanisms. Notably, the residual compression in the reinforcement can lead to an increased crack opening when the reinforcement fails, and thus a longer bridging zone. Also, the increased normal compression at the interface of the reinforcement and matrix can lead to larger frictional forces which are beneficial if pullout is limited by the length of a discontinuous reinforcement.

The foregoing examples and those summarized in Table 1 provide some guidance for the design of high toughness composites. However, these represent only a few relatively straightforward ligament extension mechanisms. Other important mechanisms include interface debonding combined with sliding and/or deformation. The sensitivity of the results in Table 1 to both the ligament separation process and the rupture condition highlights the need for a thorough understanding of the mechanics of the separation process, as well as the need for techniques to measure microscopic mechanical properties, such as interface debonding and sliding resistance, deformation of small constrained volumes, and fracture properties of small reinforcements.

ACKNOWLEDEMENTS

Funding for this work was provided by the U.S. Office of Naval Research, Contract No. N00014-85-C-0416 and Contract No. N00014-86-K-0753.

APPENDIX A

INLFUENCE OF RESIDUAL STRESS ON STRESS-DISPLACEMENT RELATION FOR FRICTIONAL BONDING

If sliding occurs between a matrix and fiber wherever the shear stress parallel to the interface exceeds a constant value τ, then application of a stress σ^o to a section of composite containing a crack in the matrix causes sliding at the interface, beginning at the crack surface and extending a distance ℓ along the fiber (Fig. A1(a)). With a shear-lag approximation in which only axial stresses σ_f exist in the fiber (shear stress concentrated at the interface), equilibrium of the fiber at $z < \ell$ requires

$$d\sigma_f/dz = 2\tau/R, \tag{A1}$$

where R is the fiber radius. If $\ell >> R$, then elastic stresses at $z > \ell$ may be neglected, and integration of Eq. (A1) with the boundary conditions indicated in Fig. A1(b) defines the sliding distance:

$$\ell = \frac{\sigma^o R}{2\tau} \frac{E_m(1 - f)}{fE} . \tag{A2}$$

The sliding displacement u_s (difference in displacements of fiber and matrix at the crack surface) is represented by the hatched area beneath the strain plots in Fig. A1(b):

$$u_s = \ell\sigma^o/2fE_f. \tag{A3}$$

The displacement to be used for the crack opening in the analysis of Sect. 2.1 has been suggested as the difference between the length, ℓ, of the fiber from the end of the sliding region to the center of the crack, and the length, ℓ', which the same section of composite would assume if sliding was prevented (Fig. A1(d)).[16,26,27] It is straightforward to show that this displacement is given by

$$u = u_s\, E_m(1 - f)/E \tag{A4}$$

Equations (A2) to (A4) combine to give

$$\sigma^o = \beta u^{1/2}, \tag{A5}$$

where

$$\beta = [4\tau f^2 E^2\, E_f/R\, E_m^2(1 - f)^2]^{1/2} \tag{A6}$$

If the residual stress σ_m^R exists intially in the matrix then the strains in the matrix and fiber are as shown in Fig. A1(c). The difference in displacement between the fibers and matrix for an applied stress σ is then given by the shaded area in Fig. A1(c), which can be expressed

$$u_s = \ell\sigma'/2f\,E_f, \tag{A7}$$

where $\sigma' = \sigma + \sigma_m^R E/E_m$. Evaluation of ℓ with the boundary conditions indicated in Fig. A1(c) gives

$$\ell = \frac{\sigma' R}{2\tau}\,\frac{E_m(1-f)}{fE}\,. \tag{A8}$$

The displacement and slip length of Eqs. (A7) and (A8) can be obtained from the corresponding values in the absence of residual stress (Eqs. (A3) and (A2)) by replacing the stress σ^o by σ', i.e.

$$\sigma + \sigma_M^R\,E/E_m = \sigma^o\,, \tag{A9}$$

which corresponds to a simple translation of the $\sigma(u)$ curve along the stress axis by $\sigma_o = -\sigma_M^R\,E/E_m$

APPENDIX B

INFLUENCE OF RESIDUAL STRESS ON TOUGHENING

The influence of residual stress on the increase in fracture energy J_B can be readily evaluated for bridging ligaments that exhibit the stress displacement law

$$\sigma^o(u) = \begin{cases} \alpha u^n & u < u_c \\ 0 & u > u_c \end{cases} . \qquad (B1)$$

In the absence of residual stress, the toughening increment is (Eqs. (2) and (B1))

$$J_B^o = 2\alpha u_c^{n+1}/(n+1) , \qquad (B2)$$

In a residually stressed composite, the stress in the ligaments is (Eqs. (12) and (B1)):

$$\sigma(u) = \begin{cases} \alpha u^n + \sigma_o & u < u^* \\ 0 & u > u^* \end{cases} \qquad (B3)$$

and the toughening increment becomes (Eqs. (2) and (B3))

$$J_B = 2u^* \sigma_o + 2 \alpha u^{*n+1}/(n + 1) \tag{B4}$$

If ligament failure ocurs at a critical displacement, $u^* = u_c$, the relative toughening becomes

$$J_B/J_B^o = 1 + (n + 1)\Sigma \tag{B5}$$

where $\Sigma = \sigma_o/Sf = -\sigma_m^R E/E_m Sf$. On the other hand, if ligament rupture occurs at a critical stress ($\sigma(u^*) = Sf$), then the relative toughening is

$$J_B/J_B^o = (1 + n\Sigma)\ (1 - \Sigma)^{1/2}. \tag{B6}$$

The variation of J_B/J_B^o over the range $|\Sigma| \leq 1$ is plotted for several values of n in Fig. B1(a) for the critical stress condition, and in Fig. B1(b) for the critical displacement condition. Clearly, the change in toughening varies dramatically with both n and the rupture criterion.

Frictionally Bonded Reinforcing Fibers

Elastic reinforcing fibers that are held in place solely by mechanical forces exhibit a stress-displacement relation given by Eq. (A5), ie, Eq. (B3) with n = 1/2. If the sliding resistance arises purely from surface roughness so that τ is not influenced by residual stresses, and if fiber failure occurs within the section of fiber between the crack surfaces, then the results of Eqs. (B5) and (B6) apply, as plotted in Fig. B1 In this case, increasing tensile residual stress in the matrix enhances the toughening for a critical stress condition (the most reasonable criterion for elastic fibers), but reduces the toughening for a critical displacement criterion. The opposite trends are evident in residual compression.

The sliding resistance could alternatively arise from Coulomb friction:

$$\tau = \mu \sigma_n \tag{B7}$$

where μ is the coefficient of sliding friction, and σ_n is the normal compressive stress at the interface between the fibers and matrix. Normal compression at the interface requires tensile residual stress in the matrix parallel to fibers:[25]

$$\sigma_m^R = \sigma_n (E_f/E + 1)\, f/(1 - f) \tag{B8}$$

With the frictional stress defined in Eq. (B7), the coefficient β in the stress-displacement relation is dependent on the residual stress (Eqs. (A6), (B7) and (B8):

$$\beta = \beta' |\sigma_o|^{1/2} \tag{B9}$$

where

$$\beta' = [4\mu f E^2 E_f / R(1 - f) E_m (E_f + E)]^{1/2} . \tag{B10}$$

Therefore, the toughness increase (Eq. (B4)) becomes

$$J_B = (\frac{4}{3}) (\frac{Sf}{\beta'})^2 (3\varepsilon/2 + 1)/|\varepsilon| \tag{B11}$$

for displacement-controlled rupture, and

$$J_B = (\frac{4}{3}) (\frac{Sf}{\beta'})^2 (1 - \varepsilon)^2 (1 + \varepsilon/2)/|\varepsilon| \tag{B12}$$

for stress-controlled rupture. Equations (B11) and (B12) are plotted in Fig. B2. In this case, the toughness is reduced by increasing tensile residual stress in the matrix for both ligament rupture criteria.

Fiber Pullout

The preceding solutions require that the fiber rupture occurs between the crack surfaces. This would occur if the fiber strength was single valued.[18] More generally, a statistical distribution of fiber strengths would permit fiber fracture at locations remote from the crack surfaces, and the broken fibers would continue to exert closure forces on the crack until they pull completely out of the matrix (Fig. 2(b)). A similar argument holds for pullout of discontinuous unbonded reinforcing fibers or interlocking grains in a polycrystalline single-phase ceramic. Specifically, for the configuration illustrated in Fig. B3, Eq. (B3) with n = 1/2 applies during initial loading, until (at stress Sf) sliding extends to the end of the fiber. Then, provided the end of the fiber is not bonded, further loading causes the fiber to pull out of the matrix (Fig. B3(b)), with a linear decrease in stress with increasing crack opening displacement, as depicted in Fig. 2(b). In a composite with frictional stresses that derive purely from surface roughness, the unloading curve is not altered by preexisting residual stresses.‡

‡ The slope of the unloading curve ($-2\pi R\tau$) is independent of σ_m^R, and at $\sigma \to 0$, the fiber is stress free, so that the intercept, D, is the relaxed length of the fiber which is also independent of preexisting residual stresses).

However, the contribution to J_B from the loading portion of the $\sigma(u)$ curve is negligible,* so that the influence of the residual stress on the fracture energy is also negligible.

In a composite with τ governed by a Coulomb friction law, the residual stress affects the slope of the unloading portion of the $\sigma(u)$ curve in Fig. 3(e) through the influence on τ of the residual stress normal to the interface. The $\sigma(u)$ relation for the unloading curve is

$$\sigma(u) = 2\pi R\tau D(1 - u/D) \tag{B13}$$

and the toughening due to bridging is (with Eqs. (2), (B7) and (B8))

$$J_B = 2\pi RD\,{}^{2}{}_{\mu}\sigma_m^R E(1 - f)/f(E_f + E) \ . \tag{B14}$$

In this case, the increase in fracture energy is proportional to the magnitude of the tensile residual stress in the matrix.

Ductile Ligaments

Deformation of ductile reinforcements that remain bonded to the elastic matrix is highly constrained, so that the stress needed to extend the ligaments exceeds the uniaxial flow stress.[23,28] The stress-displacement

* The ratio of the areas beneath the loading and unloading portions of the $\sigma(u)$ curve is $\sim u_d/D$. The displacement u_d results from elastic strains of the fiber, so that $u_d/D \sim S/E \sim 10^{-3}$.

curve is not known in detail. However, the initial portion is expected to be strongly influenced by the crack tip response at the interface, and premature ligament rupture is expected to be encouraged by the growth of voids induced by the hydrostatic stresses that develop in the constrained reinforcement. Under these conditions, the deformation should not be significantly influenced by residual stresses, and the rupture is expected to be displacement controlled. The toughening due to bridging can be written

$$J_B = J_B^C + \sigma_0 u_C. \tag{B15}$$

The toughening is thus enhanced by residual compressive stress in the matrix and reduced by residual tensile stress.

REFERENCES

1. J.J. Brennan and K.M. Prewo, "Silicon Carbide Fiber Reinforced Glass-Ceramic Matrix Composites Exhibiting High Strength and Toughness," J. Mater. Sci. 17(8), 2371-83 (1982).

2. J. Aveston, G.A. Cooper and A. Kelly, "Single and Multiple Fracture," pp. 15-26 in The Properties of Fiber Composites, Conf. Proc. Nat. Physical Lab., IPC Science and Technology Pres. Ltd., Surrey, England, 1971.

3. D.B. Marshall and A.G. Evans, "Failure Mechanisms in Ceramic-Fiber/Ceramic-Matrix Composites," J. Amer. Ceram. Soc. 68(5), 225-31 (1985).

4. R.A.J. Sambell, A. Briggs, D.C. Phillips and D.H. Bowen, "Carbon Fiber Composites with Ceramic and Glass Matrices, Part 2 - Continuous Fibers," J. Mater. Sci. 7(6), 676-81 (1972).

5. D.C. Phillips, "Interfacial Bonding and the Toughness of Carbon Fiber Reinforced Glass and Glass-Ceramics," J. Mater. Sci. 9(11), 1847-54 (1974).

6. D.B. Marshall and A.G. Evans, "Tensile Strength of Uniaxially Reinforced Ceramic Fiber Composites," in Fracture Mechanics of Ceramics, pp. 1-15, 7, Ed., R.C. Bradt, A.G. Evans, D.P.H. Hasselman and F.F. Lange, Plenum, 1986.

7. A.G. Evans, M.D. Thouless, D.B. Johnson-Walls, E. Luh and D.B. Marshall, "Some Structural P:roperties of Ceramic Matrix Fiber Composites," in Proceedings of the Fifth International Conference on Composite Materials, Ed., W.C. Harrigan and J. Strife, AIME (1985).

8. V.C. Li and I. Liang, "Fracture Processes in Concrete and Fiber Reinforced Cementitious Composites," J. Eng. Mech. 112(6), 566-586 (1986).

9. Y.W. Mai, in Applications of Fracture Mechanics to Cementitious Composites, Ed., S.P. Shah, Martinus Nijhoff, p. 399-429 (1985).

10. A.G. Evans, Z.B. Ahmed, D.G. Gilbert and P.W.R. Beaumont, "Mechanisms of Toughening in Rubber Toughened Polymers."

11. M. Ruhle, B.J. Dalgleish and A.G. Evans, "On Toughening of Ceramics by Whiskers," Scripta Met. 21(5), 681-686 (1987).

12. P.L. Swanson, C. Fairbanks, B.R. Lawn, Y-W Mai and B.J. Hockey, "Crack-Interface Bridging as a Fracture Resistance Mechanism in Ceramics: I Experimental Study," J. Am. Ceram. Soc. 70(4), 279-289

13. R. Knehans and R. Steinbrech," Memory Effect of Crack Resistance During Slow Crack Growth in Notched Al_2O_3 Bend Specimens," J. Mat. Sci. Lett. 1(8), 327-29 (1982).

14. R. Steinbrech, R. Knehans and W. Schaarwachter, "Increase of Crack Resistance During Slow Crack Growth in Al_2O_3 Bend Specimens," J. Mat. Sci. 18(1), 265-70 (1983).

15. R.F. Cook, B.R. Lawn and C.J. Fairbanks, "Microstructure-Strength Properties in Ceramics: I Effect of Crack Size on Toughness," J. Am. Ceram. Soc. 68(11), 604-15 (1985).

16. B. Budiansky, Micromechanics II, Proceedings of Tenth U.S. Congress of Applied Mechanics, 1986.

17. M.D. Thouless and A.G. Evans, "Effects of Pullout on the Mechanical Properties of Ceramic Matrix Composites," Acta. Met., in press.

18. D.B. Marshall and B.N. Cox, "Tensile Fracture of Brittle Matrix Composites: Influence of Fiber Strength," Acta. Met., in press.

19. J.R. Rice, "A Path Independent Integral and the Approximate Analysis of Strain Concentrations by Notches and Cracks," J. Appl. Mech. 35, 379-86 (1968).

20. L.R.F. Rose, "Crack Reinforcement by Distributed Springs," J. Mech. Phys. Sol., in press.

21. G.C. Sih, Handbook of Stress Intensity Factors, Lehigh University Press (1973).

22. A.G. Evans and R.M. McMeeking, "On the Toughening of Ceramics by Strong Reinforcements," Acta. Met. 34(12), 2435-2441 (1986).

23. P. Mataga and R.M. McMeeking, unpublished work.

24. L.R.F. Rose, "Effective Spring Constant for Unbroken Ligaments Between Crack Faces," in press.

25. B. Budiansky, J.W. Hutchinson and A.G. Evans, "Matrix Fracture in Fiber-Reinforced Ceramics," J. Mech. Phys. Solids 34(2), 167 (1986).

26. D.B. Marshall, B.N. Cox, B. Budiansky and A.G. Evans, "Fracture of Brittle Matrix Composites," in preparation.

27. A. Kelly and L.N. McCartney, "Matrix Cracking in Fiber-Reinforced and Laminated Composites," in Proceedings of Sixth International Conference on Composite Materials, in press.

28. L.S. Sigl, P. Mataga, B.J. Dalgleish, R. McMeeking and A.G. Evans, unpublished work.

FIGURE CAPTIONS

Fig. 1 Schematic diagram of a bridged crack showing the path used for the J-integral analysis of toughening.

Fig. 2 (a) Schematic diagram showing bridging stresses at location x within the bridging zone. (b) Stress-displacement functions for various types of bridging ligaments.

Fig. 3 Schematic diagrams showing procedure used to form a crack in a composite with residual stress.

Fig. 4 Offsets in stress-displacement law caused by residual stress.

Fig. 5 Crack surface tractions exerted by bridging zone in a material with (a) residual compression in matrix and (b) residual tension in matrix.

Fig. 6 Plots of the relative change in fracture energy due to bridging by linear springs as a function of the normalized residual stress, Σ. Positive Σ represents compressive stress in the matrix and tension in the reinforcement; negative Σ represents tension in the matrix.

Fig. 7 (a) Crack in a material with residual tensile stress in the matrix, at zero applied load, (b) pressure exerted by the bridges on the crack surfaces, and (c) stress-displacement curve for the reinforcing ligaments.

Fig. 8 Crack resistance curve for a material with residual tensile stress in the matrix, showing initial decrease due to the opening pressure exerted by bridges closest to the crack tip.

Fig. A1 Fiber pullout in frictionally-bonded composite.

Fig. B1 Variation of relative fracture energy due to bridging as a function of normalized residual stress, Σ. (a) Critical stress for ligament failure criterion and (b) critical displacement criterion.

Fig. B2 Variation of fracture energy due to bridging with normalized residual stress for reinforcements held in place by Coulomb friction.

Fig. B3 Schematic diagram showing two stages in the loading of a reinforcement that pulls entirely out of the matrix: (a) increasing $\sigma(u)$ as region over which sliding occurs extends from the crack surface towards the end of the reinforcement, and (b) decreasing $\sigma(u)$ as entire reinforcements slides out of the matrix.

Table 1

Effect of Residual Stress on Fracture Energy

Stress-Displacement Law		Rupture Condition	Residual Stress in Matrix: Tension	Residual Stress in Matrix: Compression
Linear		Stress	Decrease	Decrease
		Displacement	Decrease	Increase
Frictional (Fracture at Crack Plane)	Surface Roughness	Stress	Increase	Decrease
		Displacement	Decrease	Increase
	Coulomb Friction	Stress	Decrease	
		Displacement	Decrease	
Frictional (Pullout of Entire Reinforcement)	Surface Roughness		Negligible	Negligible
	Coulomb Friction		Increase	
Ductile	Bonded	Displacement	Decrease	Increase

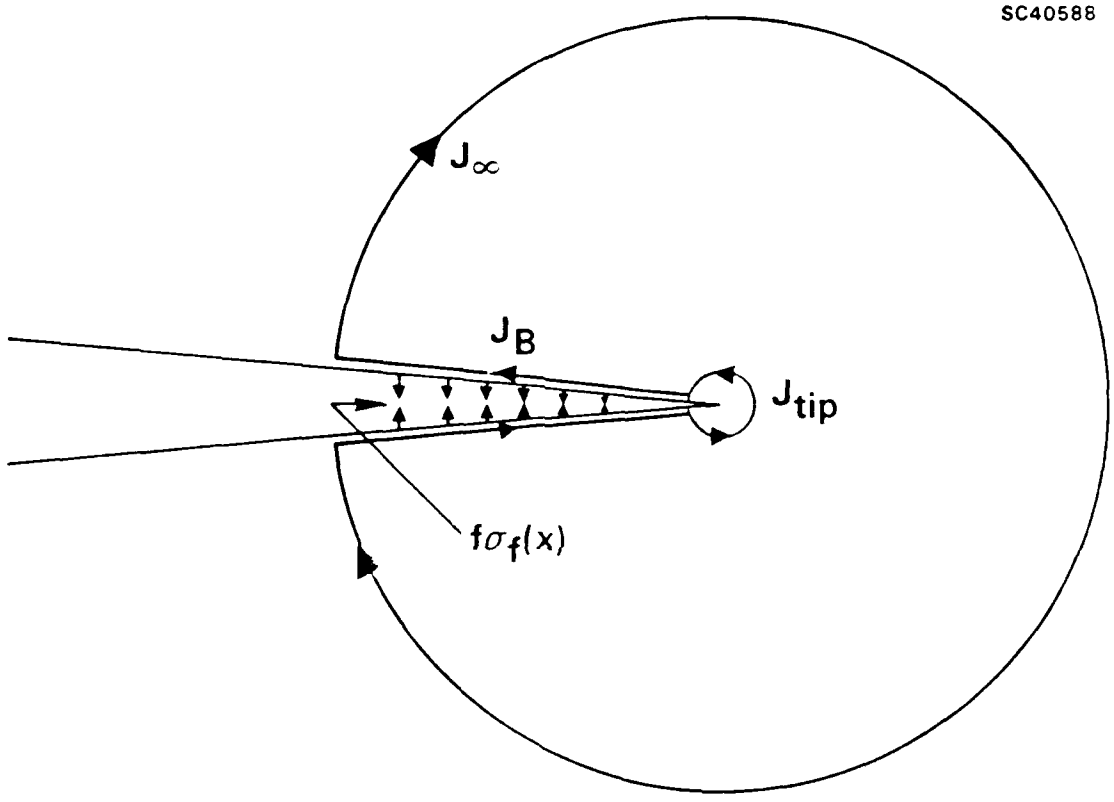
SC40588
J_∞
J_B
J_{tip}
$f\sigma_f(x)$

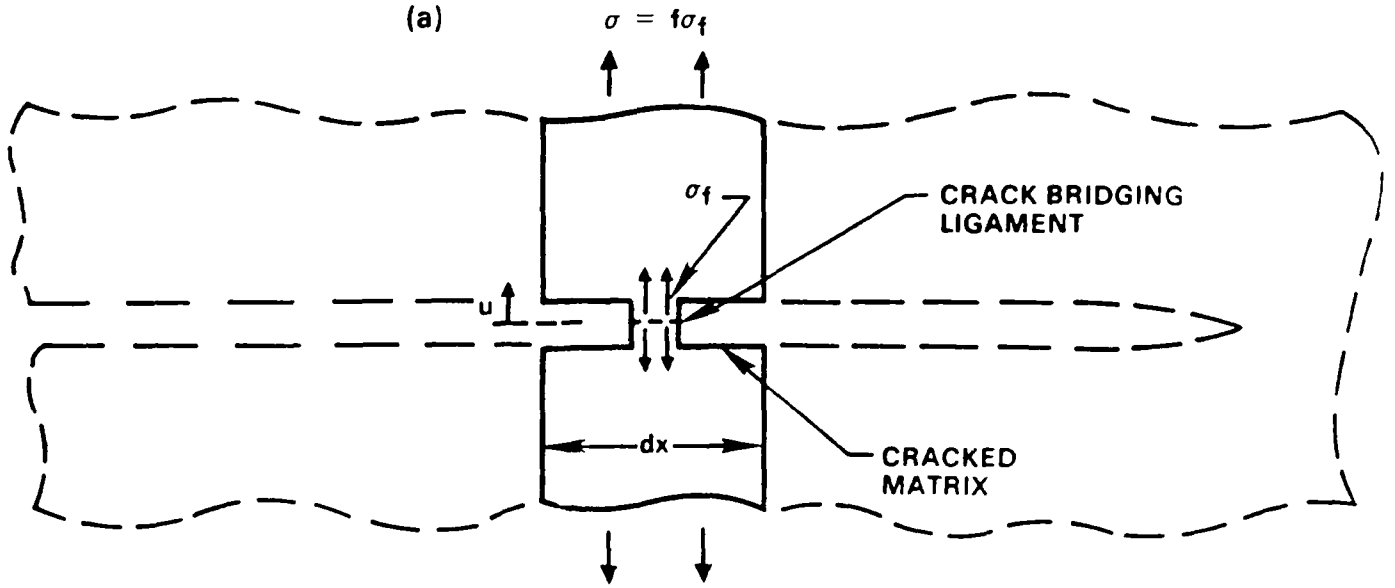
(a)
$\sigma = f\sigma_f$
σ_f
CRACK BRIDGING LIGAMENT
u
dx
CRACKED MATRIX

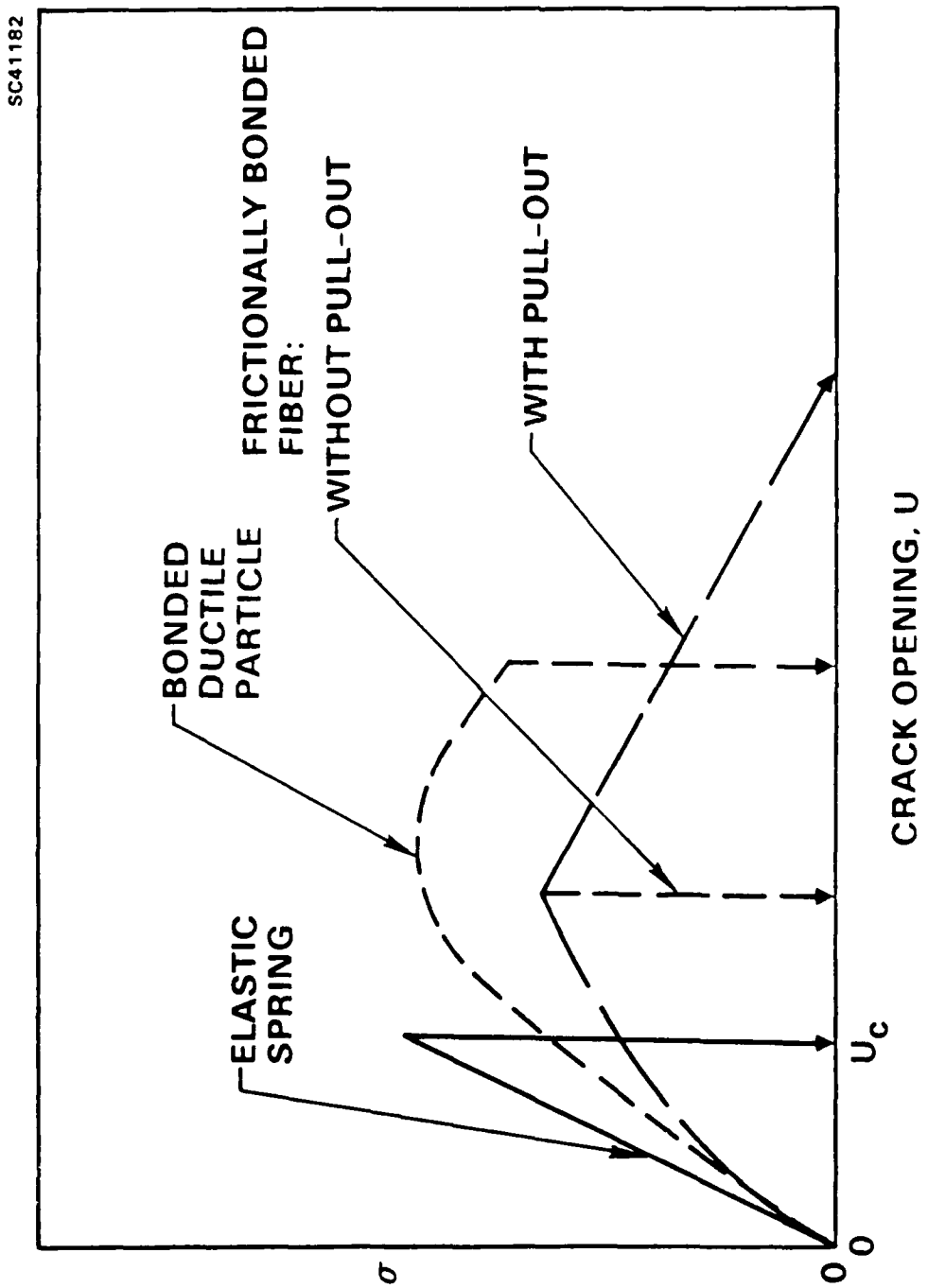
SC41182
FRICTIONALLY BONDED FIBER:
WITHOUT PULL-OUT
WITH PULL-OUT
BONDED DUCTILE PARTICLE
ELASTIC SPRING
σ
0
0
U_c
CRACK OPENING, U

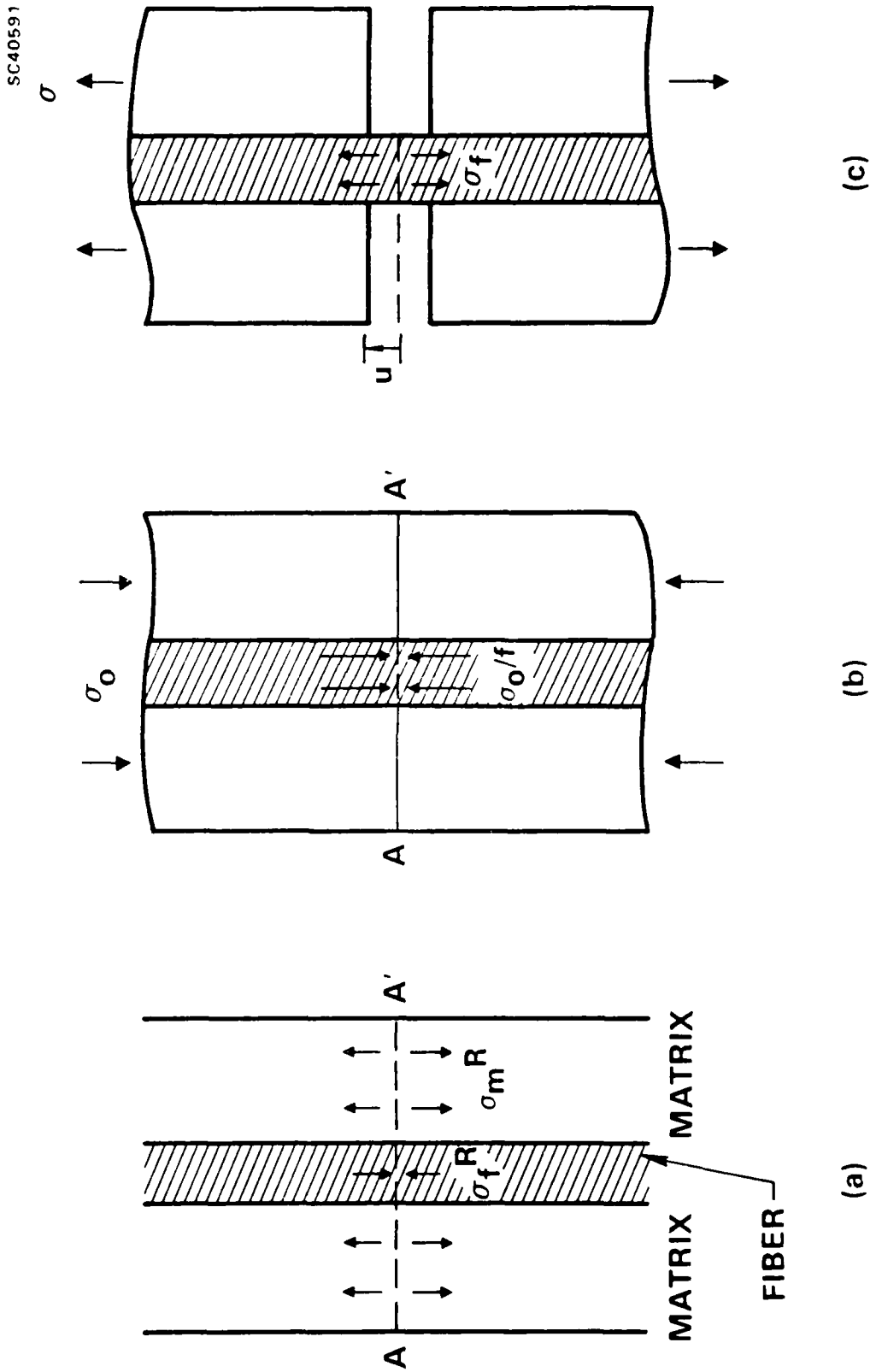
SC4059I
σ
σf
u
(c)
A'
σo
σo/f
A
(b)
A'
σmR
σfR
MATRIX
MATRIX
FIBER
A
(a)

SC41181

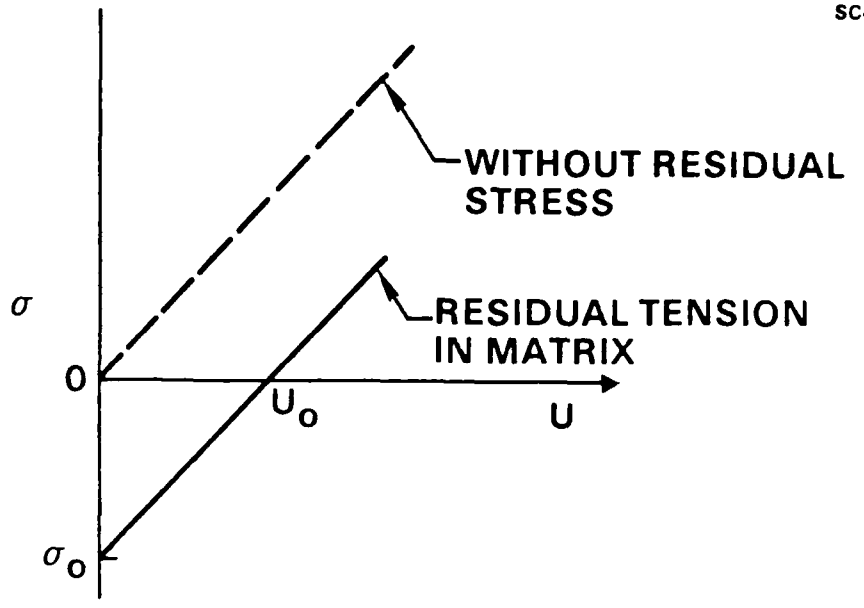
WITHOUT RESIDUAL STRESS
RESIDUAL TENSION IN MATRIX
σ
0
U_o
U
σ_o

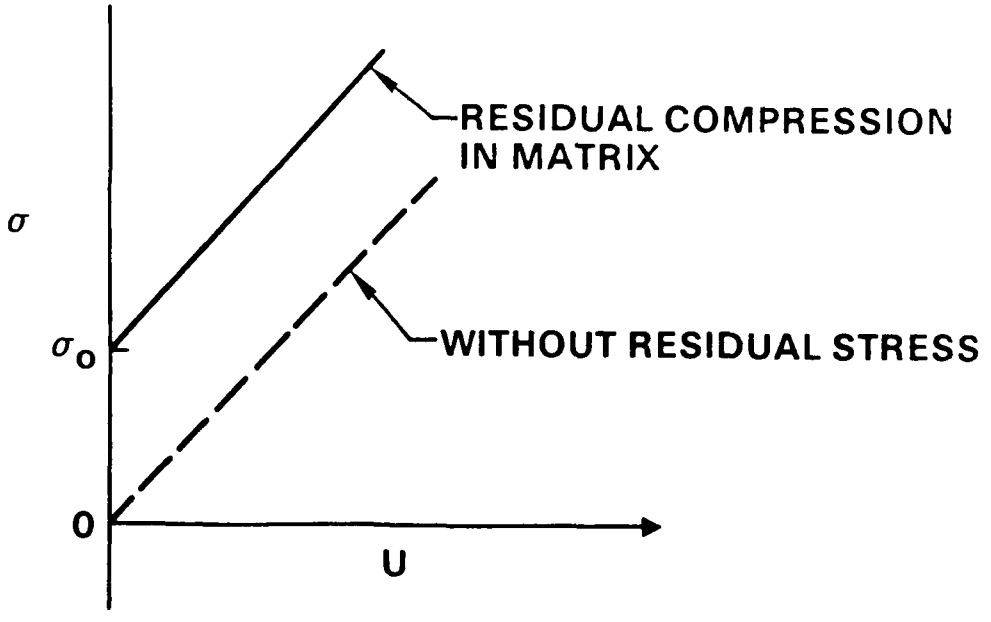
RESIDUAL COMPRESSION IN MATRIX
σ
σ_o
WITHOUT RESIDUAL STRESS
0
U

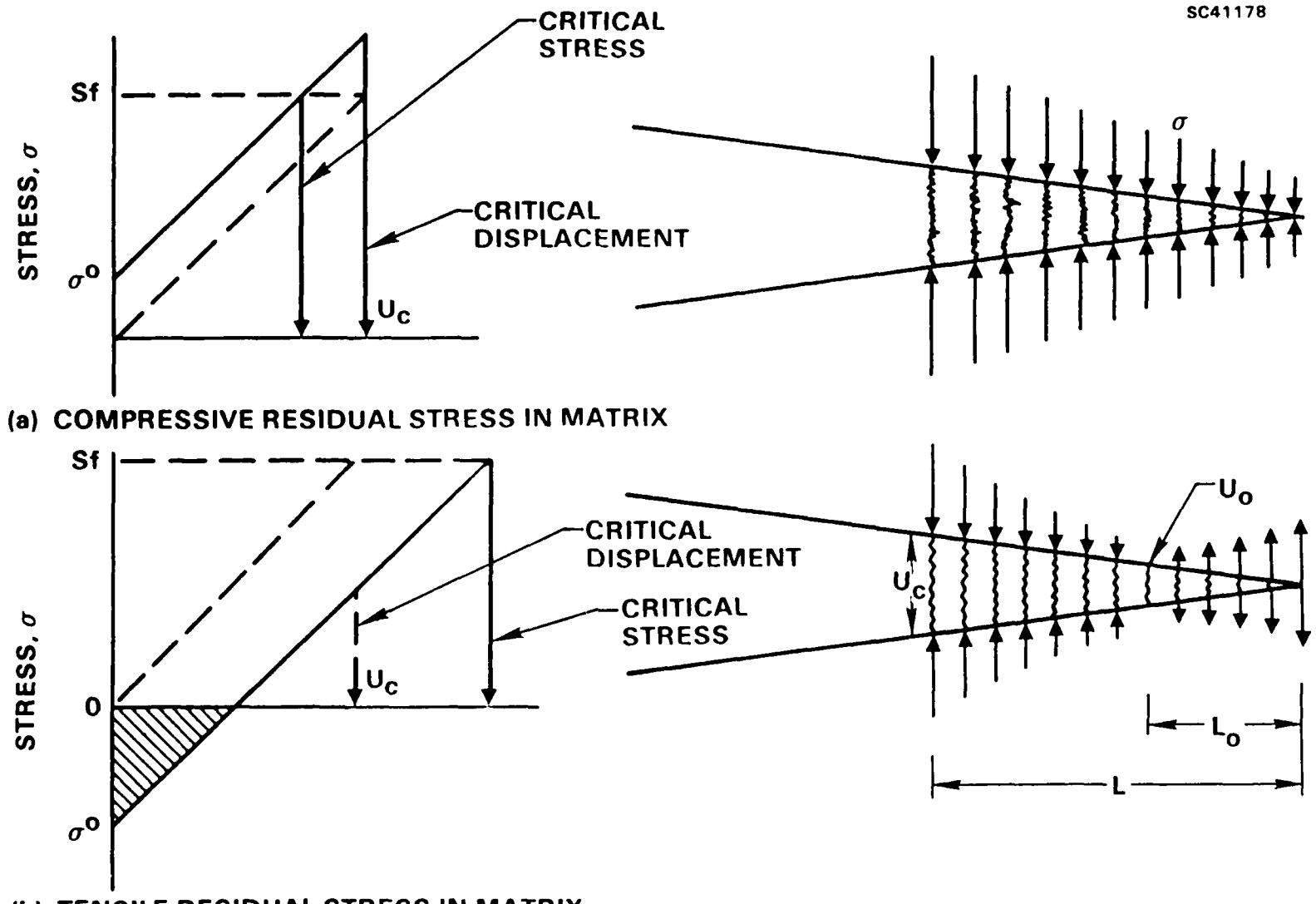
SC41178
CRITICAL STRESS
CRITICAL DISPLACEMENT
Sf
STRESS, σ
σo
Uc
σ
(a) COMPRESSIVE RESIDUAL STRESS IN MATRIX
Sf
CRITICAL DISPLACEMENT
CRITICAL STRESS
Uo
Uc
STRESS, σ
0
σo
Lo
L
(b) TENSILE RESIDUAL STRESS IN MATRIX

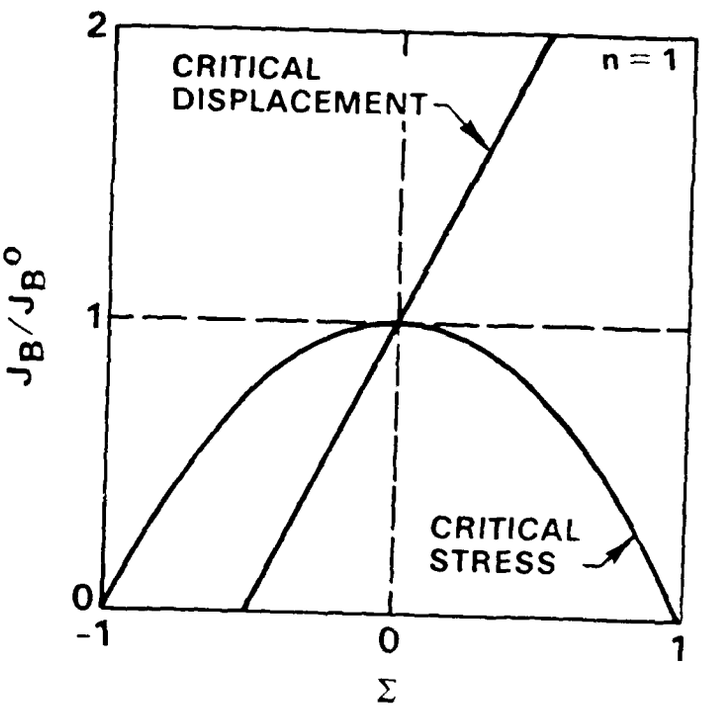
2
1
0
-1
0
1
J_B/J_B^o
Σ
CRITICAL
DISPLACEMENT
n = 1
CRITICAL
STRESS

SC40589

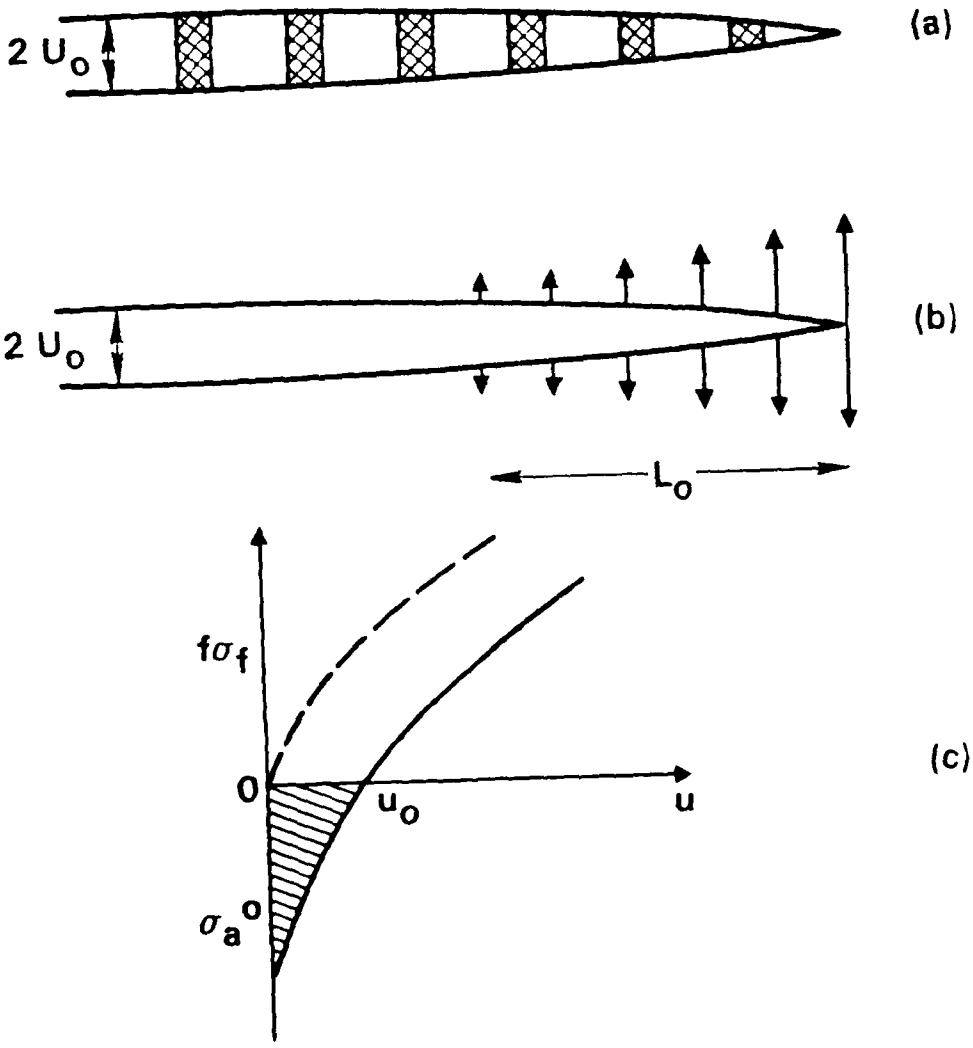

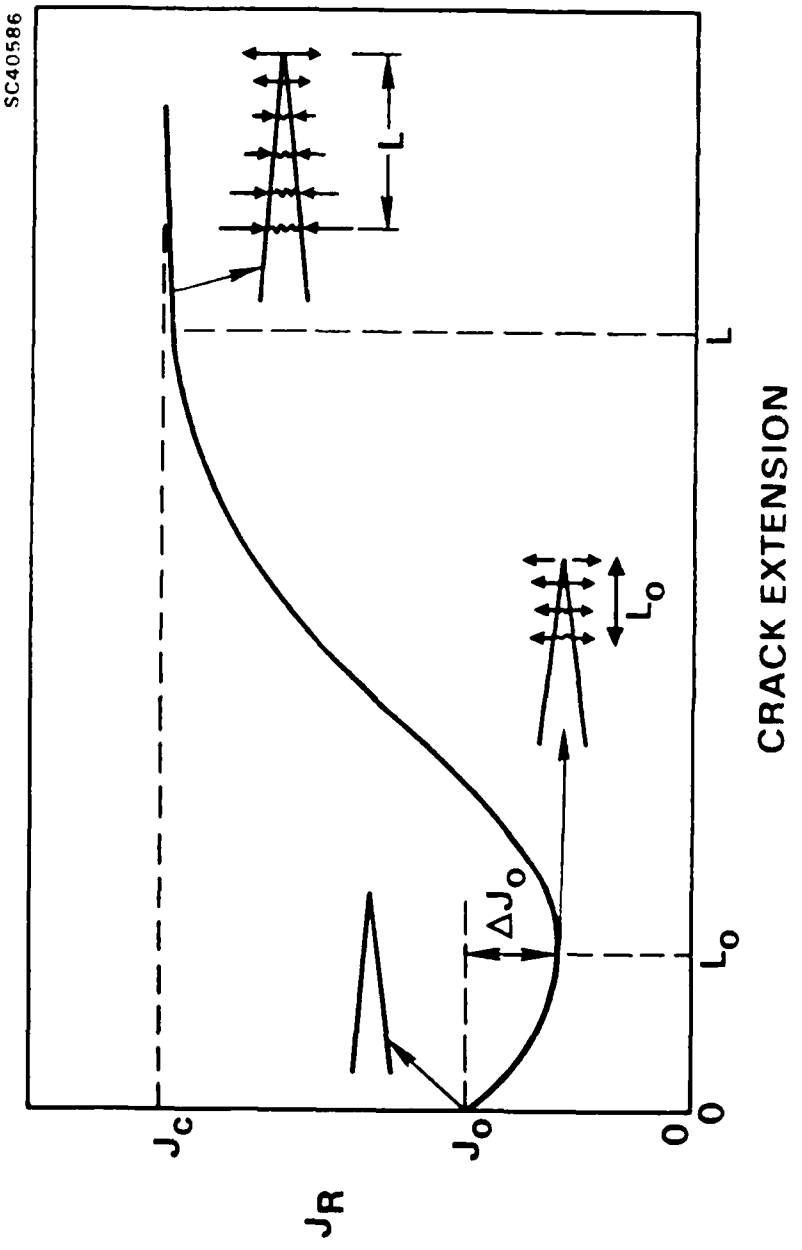
SC40586
L
L
L_o
ΔJ_o
L_o
0
J_c
J_o
J_R
CRACK EXTENSION

(a)
(b)
(c)
(d)
σ
σ/f
MATRIX
FIBER
MATRIX
FIBER
MATRIX
u
r
l
σ/E
0
STRAIN
σ/E - σ^R_m/E_m
σ/E + σ^R_f/E_f
σ/fE_f
σ_a
u'

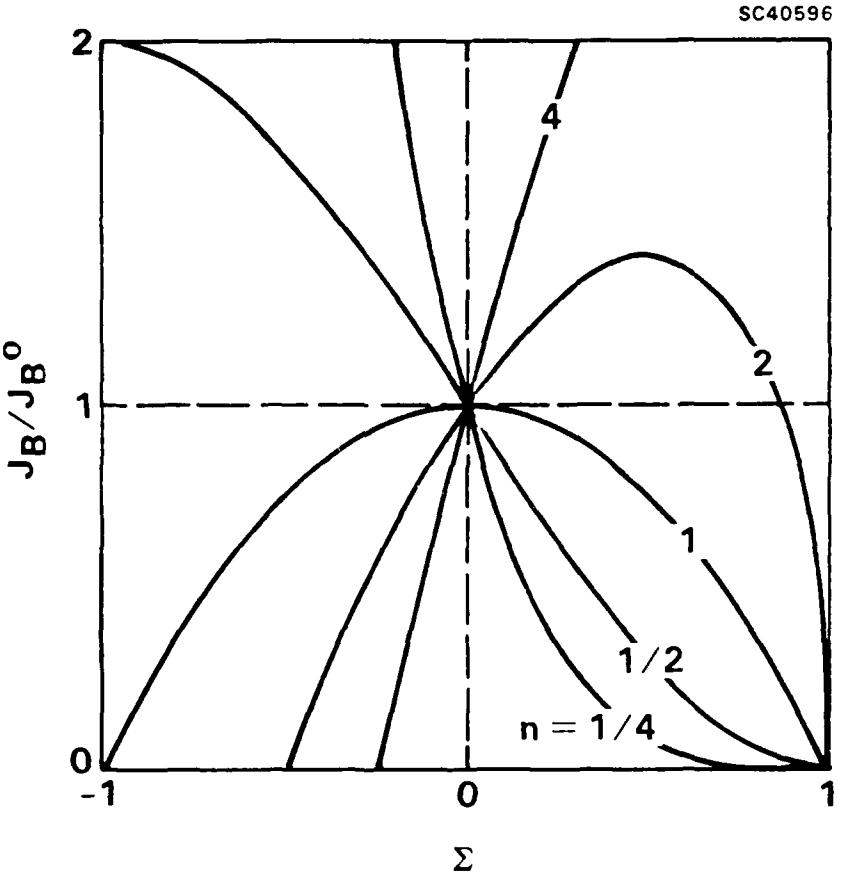
SC40596
2
1
0
-1
0
1
J_B/J_B^o
Σ
4
2
1
1/2
n = 1/4

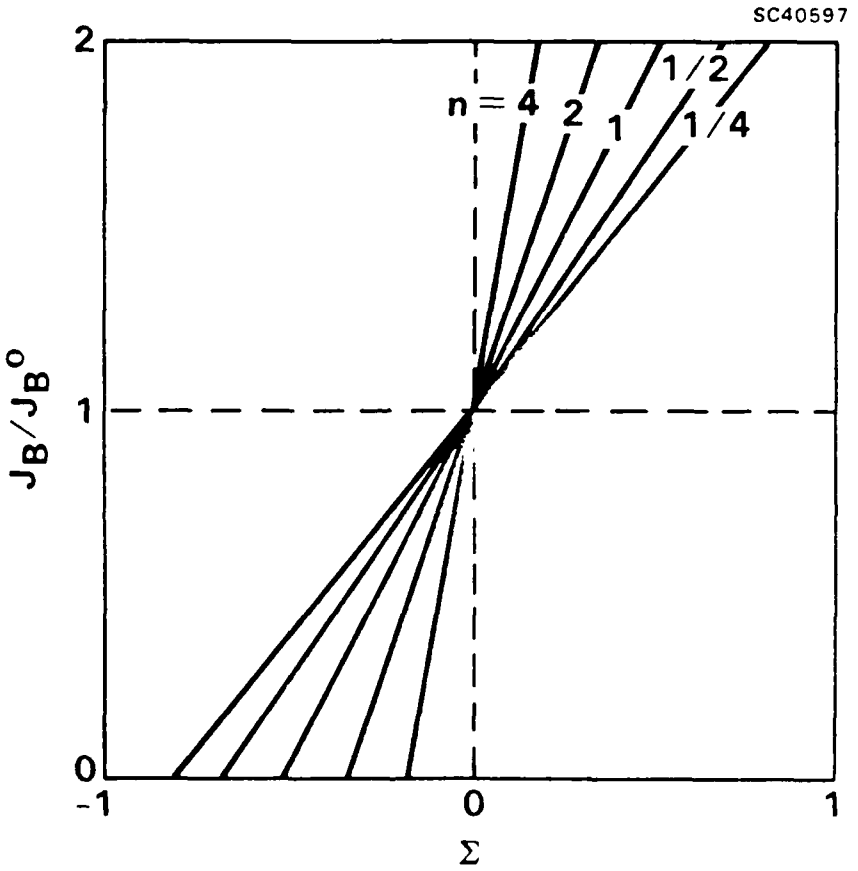
SC40597
2
1
0
-1
0
1
Σ
J_B/J_B^o
n = 4
2
1
1/2
1/4

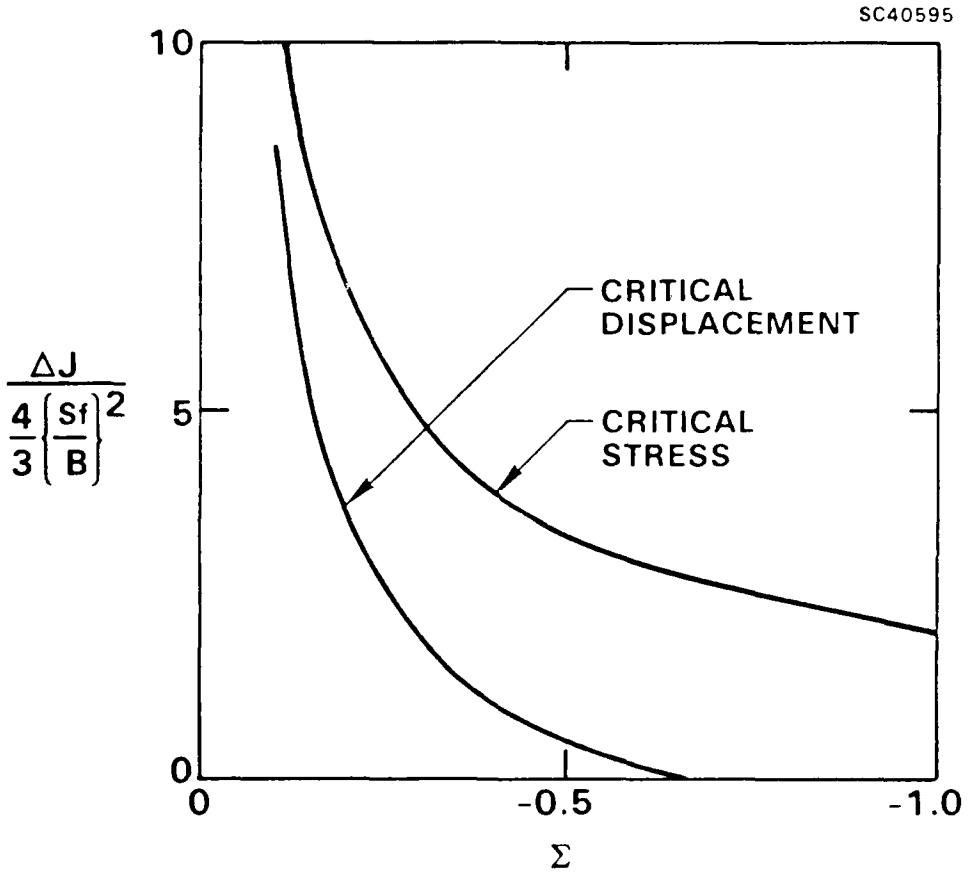
SC40595
10
5
0
0
-0.5
-1.0
Σ
ΔJ / 4/3 (Sf/B)^2
CRITICAL DISPLACEMENT
CRITICAL STRESS

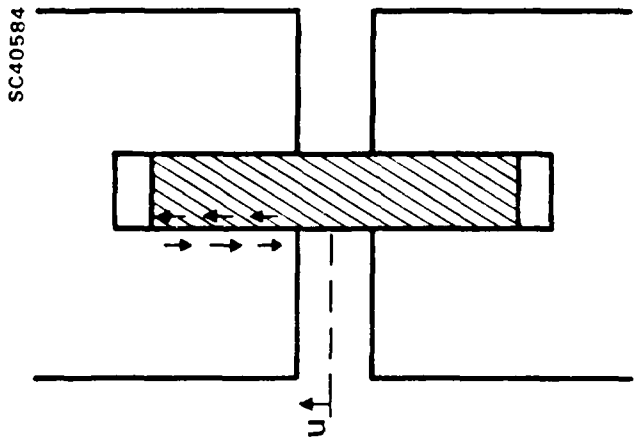
SC40584
u
PULLOUT:
DECREASING σ (u)

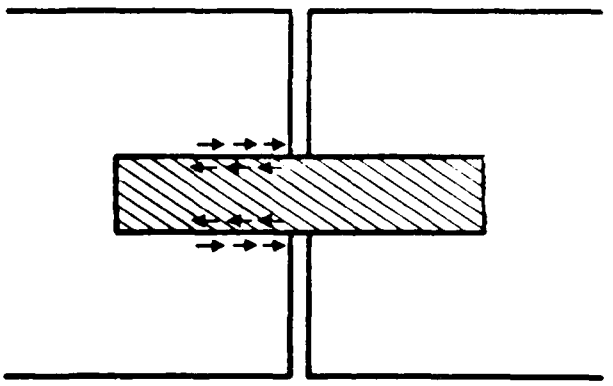
PARTIAL SLIDING:
INCREASING σ (u)

3.0 INTERFACES AND TOUGHENING IN CERAMICS

J de Physique, in press

Rockwell International
Science Center

INTERFACES AND TOUGHENING IN CERAMICS

D.B. Marshall

Rockwell International Science Center
1049 Camino Dos Rios
Thousand Oaks, CA 91360

J de Physique, in press

RESUME

La modelisation par la mecanique de la rupture a recemment fourni un eclairage approfondi du role des interfaces dans l'augmentation de la resistance a la fracture des ceramiques et des composites ceramiques par le renforcement apporte par des ponts etablissant des liens dans le defaut. Quelques resultats de la modelisation sont resumes et une methode d'indentation est decrite pour mesurer les proprietes mecaniques des interfaces (energie de decollement, resistance de frottement au glissement et contraintes residuelles) des fibres individuelles des composites en presence de liaisons faibles aux interfaces entre les fibres et la matrice.

ABSTRACT

Fracture mechanics modelling has recently provided insight into the role of interfaces in toughening of ceramics and ceramic composites by reinforcements that form crack bridging ligaments. Some results of the modelling are summarized and an indentation method is described for measuring interfacial mechanical properties (debond energy, frictional sliding resistance, and residual stresses) at individual fibers in composites with weak interfacial bonding between the fibers and matrix.

1.0 INTRODUCTION

Brittle materials can be substantially toughened by reinforcements that form ligaments between crack surfaces. This toughening mechanism has been demonstrated in large-grained single phase ceramics such as Al_2O_3[1,2] as well as in fiber,[3-5] whisker[6] and metal[7] reinforced ceramic composites. In all of these examples the properties of the interface between the reinforcement and the matrix play a critical role in determining the extent of toughening.

The purpose of this paper is to examine some of the properties of the interface that need to be characterized in order to design optimum mechanical properties of the composite. First some recent developments in fracture mechanics analysis will be summarized. These demonstrate a means of obtaining the relation between macroscopic properties (e.g., strength, fracture toughness) and the micromechanical behavior of the crack-bridging ligaments, as influenced by interfacial properties and residual stresses. Some results are presented for a specific composite that has bridging ligaments dominated by frictional sliding. Then an indentation method which allows some of the important properties such as interfacial debonding, frictional forces and residual stresses to be measured directly at individual fibers is described.

2. TOUGHENING BY BRIDGING

2.1 Fracture Mechanics Analysis

Two approaches have been developed recently to analyze the influence of bridging ligaments on the toughening of ceramics. Both model the bridging ligaments as closure tractions acting on the crack surfaces within the bridging zone (Fig. 1). In one approach[8,9] the modified crack tip stresses are calculated directly using a standard Green's function, analogous to the Dugdale/Barenblatt models of fracture.[10,11] However, these models assume uniform closure tractions within the bridging zone and a failure criterion defined by allowing the stress singularities due to the applied loading and the bridging forces to cancel. More generally, the closure tractions must exhibit a dependence upon the crack opening displacements, characteristic of the particular reinforcing mechanism. Moreover, the usual stress singularity exists in the matrix near the tip of the crack, with stress intensity factor equal to the toughness of the unreinforced matrix. Evaluation of the influence of the bridging forces in this case requires solution for the crack opening displacement as a function of position within the bridging zone. With the exception of a few special cases, this requires numerical solution of an integral equation.

An alternative, equivalent approach involves use of the J-integral.[12-14] Based on this formulation, the increase in fracture energy is given by

$$\Delta J = 2 \int_0^{u^*} \sigma(u)\, du \qquad (1)$$

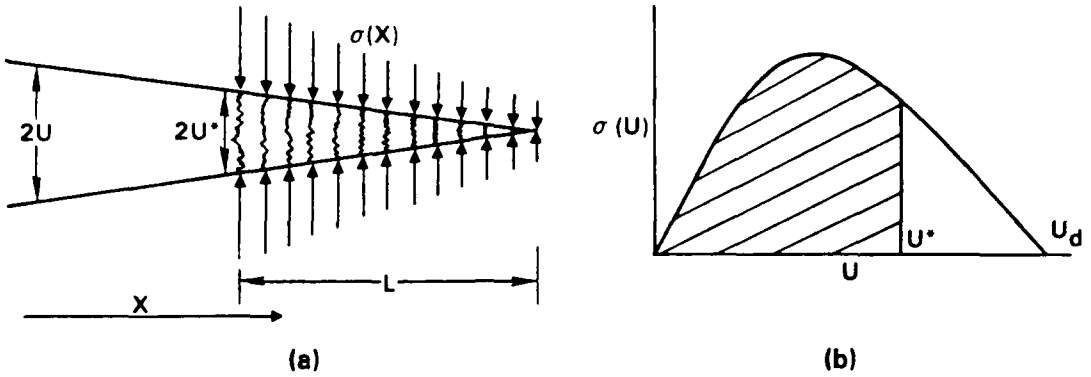

Fig. 1 (a) Closure tractions exerted by crack bridging ligaments, (b) stress-displacement relation for stretching of bridging ligaments.

where $\sigma(u)$ is the stress-displacement relation for stretching the bridging ligaments, u is the crack opening displacement and u* the crack opening at the end of the bridging zone. For general initial crack configurations it is necessary to solve for u as a function of position in the crack, as in the stress intensity approach, in order to evaluate u*. However, for the special case of steady-state toughening, defined by $u^* = u_d$, where u_d is the crack opening above which the ligaments cease to restrain the crack surfaces, the toughening is given simply by the area beneath the $\sigma(u)$ curve and solution for the crack opening displacements is not necessary.

In both of these analyses the properties of the reinforcement and the interface between the reinforcement and the matrix influence the macroscopic fracture properties through the stress-displacement function for ligament stretching. Some stress-displacement functions for brittle and ductile reinforcements are illustrated in Fig. 2. For brittle reinforcements with interfaces bonded sufficiently strongly to prevent debonding when a crack passes, the area beneath the $\sigma(u)$ curve is relatively small. Weak interfaces that allow some debonding result in more compliant ligaments with the possibility of ligament failure within the region of ligament embedded in the matrix, frictional pullout, and large steady-state toughening. Reinforcements held in place by mechanical forces without chemical bonding allow the largest toughening. On the other hand, ductile reinforcements appear to exhibit maximum toughening when the interface between the reinforcement and matrix is strongly bonded.[7] If debonding occurs the bridging stress is limited to the uniaxial flow stress of the ligament material, whereas in a fully-bonded ductile particle, elastic constraint due to the matrix can lead to bridging stresses exceeding the uniaxial flow stress by nearly an order of magnitude.[7]

Residual microstructural stresses, which are often unavoidable in composites, influence the macroscopic toughening by modifying the $\sigma(u)$ function for the bridging ligaments.[13] For several important bridging mechanisms this involves simply translation of the $\sigma(u)$ function along the stress axis. However, the resultant effect on the steady-state toughening is very sensitive (in both sign and magnitude) to both the functional form of the $\sigma(u)$ relation and the rupture criterion for the ligaments. Calculated trends for several types of bridging mechanisms are summarized in Table 1.[13]

2.2 Unbonded Reinforcements

The use of fracture mechanics to relate macroscopic composite properties to reinforcement interface properties can be illustrated by examining the behavior of composites containing unbonded reinforcements that are held in place by mechanical forces. This system has been analyzed in detail using both of the above approaches.[8,9] Examples of such composites include glass and glass-ceramic matrices reinforced by graphite and SiC fibers.[3,4] The macroscopic fracture behavior of these composites can vary dramatically, depending on the magnitude of the sliding resistance at the interface. For sufficiently high frictional stress failure occurs by growth of a single crack. Then a steady-state fracture toughness, K_c, can be defined:[9]

$$K_c/K_0 = (E/E_m)\ (1 + \alpha)^{1/2} \qquad (2)$$

with

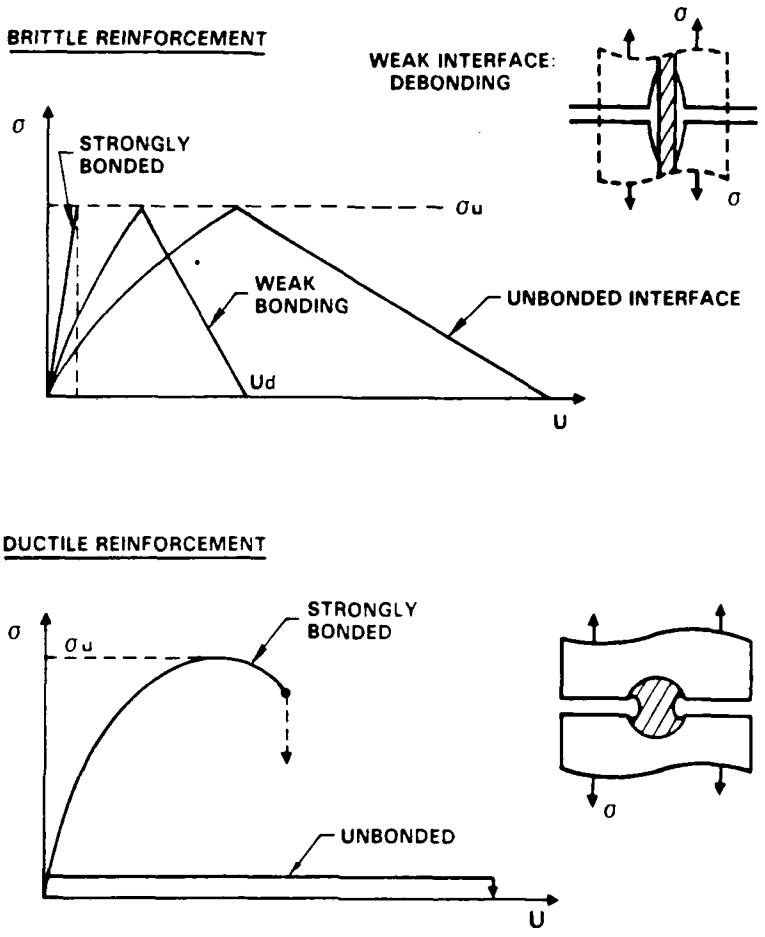

Fig. 2 Schematic stress-displacement relations for stretching of brittle and ductile reinforcements.

$$\alpha = \frac{S^3 R f (1 - f) E_m^3}{3(1 - \nu^2)\tau E_f E^2 K_0^2} \quad , \tag{3}$$

where τ is the frictional stress that resists sliding at the interface, R is the fiber radius, S is the strength of the fiber, K_0 is the toughness of the unreinforced matrix, f is the volume fraction of fibers, E_f, E_m, and E are the Young's moduli of the fibers, matrix and composite, and ν is Poisson's ratio of the composite. Therefore, it is evident that decreasing the frictional stress increases the steady-state toughness. However, if τ decreases below a critical value defined by $\alpha = 1$, a change in fracture mechanism can occur. A crack that is initially bridged by fibers can extend entirely through the matrix without any of the bridging fibers fracturing. The composite does not fail catastrophically, but instead can support further load increase (nonlinear) before failure. The stress for matrix cracking is then an intrinsic property of the composite (i.e., independent of flaw size) given by[5,8,9,15]

$$\sigma_0 = \left[\frac{6(1 - \nu^2)\,\tau f^2 E_f E K_0^2}{R\, E_m^3 (1 - f)} \right]^{1/3} \tag{4}$$

Table 1
Effect of Residual Stress on Fracture Energy

Stress-Displacement Law		Rupture Condition	Residual Stress in Matrix: Tension	Residual Stress in Matrix: Compression
Linear		Stress	Decrease	Decrease
		Displacement	Decrease	Increase
Frictional (Fracture at Crack Plane)	Surface Roughness	Stress	Increase	Decrease
		Displacement	Decrease	Increase
	Coulomb Friction	Stress	Decrease	
		Displacement	Decrease	
Frictional (Pullout of Entire Reinforcement)	Surface Roughness		Negligible	Negligible
	Coulomb Friction		Increase	
Ductile	Bonded	Displacement	Decrease	Increase

In this region of behavior, decreasing τ causes σ_0 to decrease. Therefore, optimum values of σ_0 or ΔK are achieved at an intermediate value of τ corresponding to the transition in failure mechanism ($\alpha \sim 1$).

3. MEASUREMENT OF INTERFACIAL MECHANICAL PROPERTIES

An indentation technique has been developed recently to allow measurement of frictional sliding resistance and debond fracture energy at individual fibers in weakly bonded composites.[16,17] Analysis is also presented below to enable the method to be used to measure the magnitude of residual stress in the fibers.

The method entails loading a sharp indenter (e.g., Vickers hardness pyramid) onto the end of a fiber in a polished cross section of the composite and measuring the applied force and displacement continuously (Fig. 3). If this loading causes debonding at the fiber-matrix interface with frictional sliding over the debonded area, the displacement of the fiber relative to the matrix surface is

$$u = F^2/4\pi^2R^3\tau E_f - 2\Gamma/\tau \qquad (5)$$

where F is the force applied to the fiber and Γ is the debond fracture energy (Mode II). The displacement measured in these experiments is the sum of the sliding distance given by Eq. (5) and the penetration of the indenter (elastic and plastic) into the fiber (Fig. 3a). The penetration must be either calculated or (preferably) calibrated in separate experiments where fiber sliding does not occur. The calibration has been obtained in a SiC/glass-ceramic composite by heat treating the composite in air at 1000°C to form a strongly bonded oxide layer at the fiber-matrix interface which does not debond during indentation.[17] Measurements in the as-fabricated composite indicated that sliding occurred between the fiber and matrix (Fig. 3b). The measured sliding distances for this composite are compared with the predictions of Eq. (5) in Fig. 4a. The data follow a linear relation when plotted as F^2 versus u as predicted, with intercept $2\Gamma/\tau = 0 \pm 0.01$ μm. Measured values of peak force and displacements, $F_m = 0.11$ N and $u_m = 0.80$ μm with R = 8.0 μm and $E_f = 200$ GPa, gave $\tau = 3.5$ MPa and an upper bound for the debond fracture energy (defined by the experimental errors) of $0.04 \cdot J\ m^{-2}$. Therefore, the debond fracture energy in this composite is very small (smaller than that expected for Van der Waals force) and the mechanical response of the crack bridging ligaments is dominated by mechanical sliding resistance.

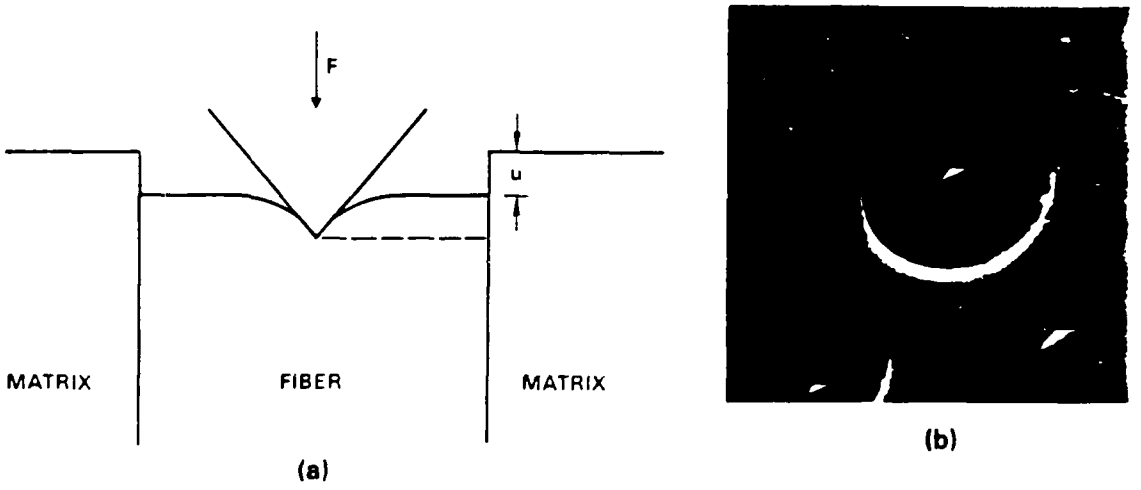

Fig. 3 (a) Indentation method for measuring frictional sliding resistance, and (b) scanning electron micrograph showing SiC fibers in glass-ceramic matrix after indentation with a diamond pyramid (triangular based). From Ref. 17.

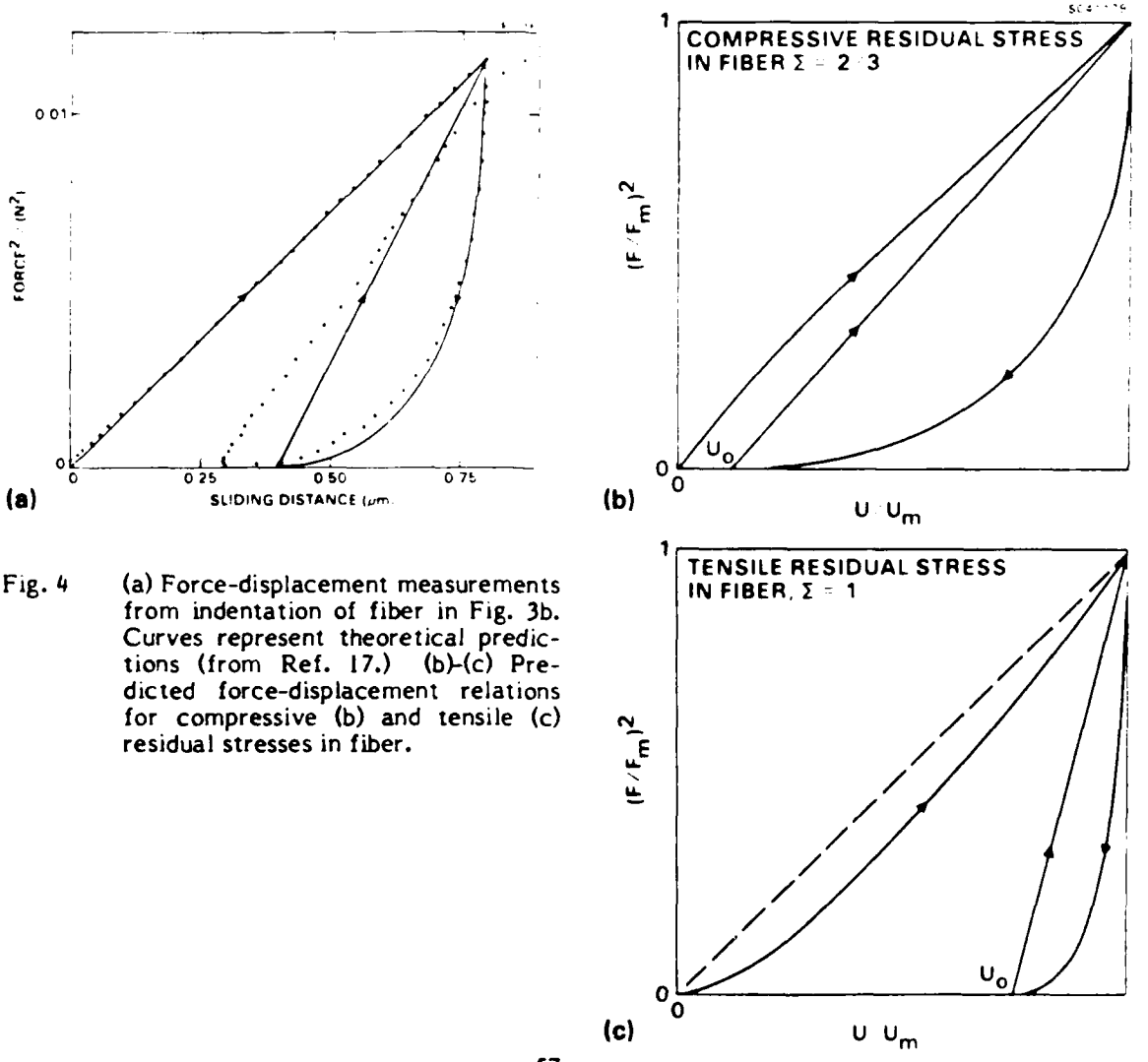

Fig. 4 (a) Force-displacement measurements from indentation of fiber in Fig. 3b. Curves represent theoretical predictions (from Ref. 17.) (b)-(c) Predicted force-displacement relations for compressive (b) and tensile (c) residual stresses in fiber.

Force-displacement measurements for unloading and reloading are also shown in Fig. 4a. Analysis of fiber sliding, assuming constant frictional stress, τ, and no bonding, predicts the displacements[16]

$$u/u_m = 1 - (1 - F/F_m)^2/2 \tag{6}$$

and

$$u/u_m = 1 + (F/F_m)^2/2 \tag{7}$$

for unloading and reloading. The measured fiber displacement after unloading is smaller than predicted, suggesting that the sliding resistance during reverse slip was lower than during the initial slip by about 20%.[17]

The sliding distances in these experiments are modified if residual stresses exist in the composite. Compressive residual stress in the fiber causes the plot of F^2 versus u to be changed as shown in Fig. 4b: the initial loading curve is nonlinear, with decreasing slope with increasing F, the residual displacement, u_o, after unloading is smaller than the value $u_o = u_m/2$ obtained in the absence of residual stress, and the reloading curve is linear. The residual displacement u_o for an unloaded system with constant τ during forward and reverse sliding is

$$u_o/u_m = 1 - 1/2\ [1 - \Sigma(1 - \Sigma/2)] \tag{8}$$

where

$$\Sigma = 2\pi R^2 \sigma_R/F_m \quad . \tag{9}$$

The magnitude of the residual stress may be calculated from measurement of u_o. Caution is required, however, for values of u_o less than 0.5 can also be caused by the need to debond the interface before sliding can occur, or by a decrease in τ during reverse sliding as observed in Fig. 4a. The three potential causes for residual displacements to be less than $u_m/2$ can be distinguished by their different influences on the initial loading curve.

For tensile residual stress in the fiber, the force-displacement curve is modified as in Fig. 4c: the initial loading curve has curvature opposite to that caused by compressive stress, the residual displacement after unloading is larger than $u_m/2$, and the reloading curve is again linear. The residual displacement, u_o, is given by

$$u_o/u_m = 1 - 1/2(1 + \Sigma) \tag{10}$$

and the magnitude of the residual stress may be calculated from measurement of u_o.

4. CONCLUSIONS

The amount of toughening achieved in ceramics with reinforcements that form crack-bridging ligaments is very strongly dependent on the nature of the interface between the reinforcement and matrix and its influence on the stress-displacement relation for ligament stretching. Important properties are debonding resistance, frictional sliding resistance and residual stresses. For brittle reinforcements enhanced toughening is obtained with weak, or no interfacial bonding, low frictional stresses, and tensile or compressive residual stresses in the matrix depending on the specific stress-displacement law for the bridging ligaments. For ductile ligaments large toughening is achieved with strong interfacial bonding and compressive residual stress in the matrix. Because of the sensitivity of both the magnitude and sign of toughening to the specific stress-displacement law, it is critical to develop methods for measuring interfacial mechanical properties. For weakly bonded brittle reinforcements, the indentation method provides quantitative measurements of debond energy, frictional sliding stress and residual stress at individual fibers.

5. ACKNOWLEDGEMENT

Funding for this work was provided by the U.S. Office of Naval Research, Contract No. N00014-85-C-0416. Most of the work summarized here was done in collaboration with B.N. Cox, A.G. Evans and W.C. Oliver, and benefitted from discussions with B. Budiansky and B.R. Lawn.

6. REFERENCES

1. P.L. Swanson, C. Fairbanks, B.R. Lawn, Y-W Mai and B.J. Hockey, "Crack-Interface Bridging as a Fracture Resistance Mechanism in Ceramics: I Experimental Study," J. Am. Ceram. Soc. 70(4), 279-289.

2. R. Knehans and R. Steinbrech, "Memory Effect of Crack Resistance During Slow Crack Growth in Notched Al_2O_3 Bend Specimens," J. Mat. Sci. Lett. 1(8), 327-29 (1982).

3. J.J. Brennan and K.M. Prewo, "Silicon Carbide Fiber Reinforced Glass-Ceramic Matrix Composites Exhibiting High Strength and Toughness," J. Mater. Sci. 17(8), 2371-83 (1982).

4. R.A.J. Sambell, A. Briggs, D.C. Phillips and D.H. Bowen, "Carbon Fiber Composites with Ceramic and Glass Matrices, Part 2 - Continuous Fibers," J. Mater. Sci. 7(6), 676-81 (1972).

5. D.B. Marshall and A.G. Evans, "Failure Mechanisms in Ceramic-Fiber/Ceramic-Matrix Composites," J. Amer. Ceram. Soc. 68(5), 225-31 (1985).

6. M. Rühle, B.J. Dalgleish and A.G. Evans, "On Toughening of Ceramics by Whiskers," Scripta Met. 21(5), 681-686 (1987).

7. A.G. Evans and R.M. McMeeking, "On the Toughening of Ceramics by Strong Reinforcements," Acta. Met. 34[12] 2435-2441 (1986).

8. D.B. Marshall and A.G. Evans, "Tensile Strength of Uniaxially Reinforced Ceramic Fiber Composites," in Fracture Mechanics of Ceramics, pp. 1-15, 7, Eds., R.C. Bradt, A.G. Evans, D.P.H. Hasselman and F.F. Lange, Plenum, 1986.

9. D.B. Marshall and B.N. Cox, "Tensile Fracture of Brittle Matrix Composites: Influence of Fiber Strength," Acta. Met., in press.

10. D.S. Dugdale, "Yielding of Steel Sheets Containing Slits," J. Mech. Phys. Solids 8, 100 (1960).

11. G.I. Barenblatt, "The Mathematical Theory of Equilibrium Cracks in Brittle Fracture," Adv. Appl. Mech. 7 55 (1962).

12. B. Budiansky, Micromechanics II, Proceedings of Tenth U.S. Congress of Applied Mechanics, 1986.

13. L.R.F. Rose, "Crack Reinforcement by Distributed Springs," J. Mech. Phys. Sol., in press.

14. D.B. Marshall and A.G. Evans, "The Influence of Residual Stress on the Toughness of Reinforced Brittle Materials," Materials Forum, in press.

15. J. Aveston, G.A. Cooper and A. Kelly, "Single and Multiple Fracture," pp. 15-26 in The Properties of Fiber Composites, Conf. Proc. Nat. Physical Lab., IPC Science and Technology Pres. Ltd., Surrey, England, 1971.

16. D.B. Marshall, "An Indentation Method for Measuring Matrix-Fiber Frictional Stresses in Ceramic Composites," J. Am. Ceram. Soc. 67[12] C259-60 (1984).

17. D.B. Marshall and W.C. Oliver, "Measurement of Interfacial Mechanical Properties in Fiber-Reinforced Ceramic Composites," J. Am. Ceram. Soc. in press.

SC5432.AR

4.0 NDE OF FIBER AND WHISKER-REINFORCED CERAMICS

Published in Review of Progress in Quantitative Nondestructive Evaluation, Vol. 6B, ed., D.O. Thompson and D.E. Chimenti, Plenum, 1987.

NDE OF FIBER AND WHISKER-REINFORCED CERAMICS

D.B. Marshall
Rockwell International Science Center
Thousand Oaks, CA 91360

1. INTRODUCTION

The use of nondestructive evaluation (NDE) to predict strength or reliability of materials requires two steps. One is to identify and measure the dimensions of strength-controlling defects, and the other is to relate the defect size to the strength. The purpose of this paper is to examine such relations between defects and strength for ceramic fiber composites, and to identify some of the important flaws for which nondestructive detection methods will be needed.

Because of their low intrinsic fracture toughness, the strengths of ceramics are generally very sensitive to defects. For uniform fine-grained materials such as Si_3N_4, well-defined relations have been established between the strength and sizes of various types of defects, such as cracks, voids and inclusions. Since strength generally decreases with increasing defect size, NDE requires a search for the largest defect. The surface crack is the most severe type of flaw for a given size and has accordingly received most attention [1-5]. However, well-defined relations between strength and preexisting flaw size do not always exist. For example, in materials that exhibit crack resistance curve behavior, the crack that causes failure changes in size as load is applied to the body, and may even nucleate during loading [6,7]. Then, strength is dictated by the microstructural characteristics that determine the shape of the resistance curve, rather than by preexisting flaws. In ceramic composites, a further complication arises from the possibility of several failure mechanisms, depending on the microstructure of the composite and the applied stress state [8,9]. Nevertheless, by combining direct observations of failure mechanisms and micromechanical fracture analysis, relations between defects and strength can be obtained [10-16]. In the following sections, such relations will be examined, with specific reference to composites composed of glass and glass ceramics reinforced by continuous SiC fibers [17]. However, many of the mechanisms are expected to be common to other brittle matrix composites.

2. UNIAXIALLY REINFORCED COMPOSITES

Tensile strength and toughness of materials that are inherently brittle can be dramatically improved by fiber and whisker reinforcement

in "Progress in Quantitative NDE" Plenum 1986

[17]. This generally requires weak interfaces between the fibers and matrix to allow debonding and sliding near the tips of cracks. However, this requirement also leads to anisotropy in uniaxially reinforced composites, with improved tensile properties parallel to the fibers, but severely degraded transverse and shear properties.

2.1 Tensile Loading

Two basically different failure mechanisms have been identified in uniaxially reinforced composites that are loaded in tension parallel to the fibers [8]. The corresponding load-deflection curves are illustrated in Fig. 1. If the fibers are not sufficiently "strong" (a concept that will be defined later), then failure is catastrophic. On the other hand, for high-strength fibers, the failure may be noncatastrophic, with a nonlinear loading response and gradual decrease in load-carrying capacity beyond the peak. The noncatastrophic decrease in load gives the material the appearance of being very tough. Load deflection curves of this form have been reported in glasses and glass ceramics reinforced by carbon and SiC fibers [17-20].

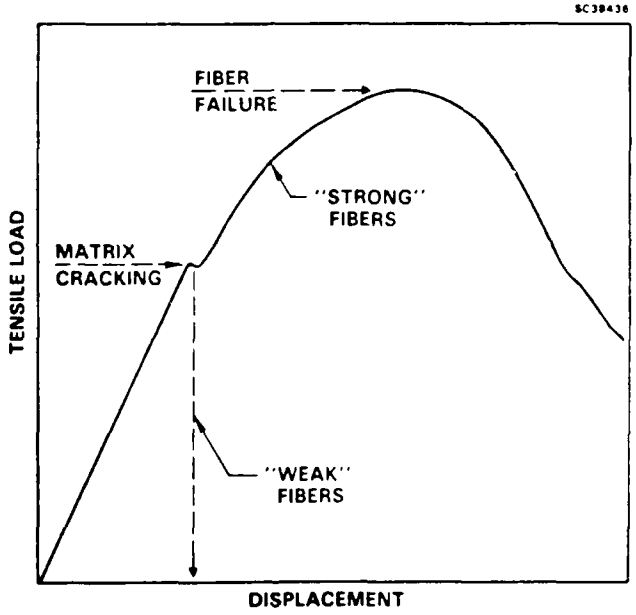

Fig. 1 Load-deflection responses for ceramic composites.

High-Strength Fibers. The noncatastrophic failure mode is characterized by the formation of periodic cracks that extend completely through the matrix without causing fiber breakage [8,11]. The formation of the first of these cracks coincides with the onset of the nonlinear load-deflection, and the multiple cracking occurs during further load increase. Fracture mechanics modeling has predicted that the first matrix crack forms at a stress that is independent of the size of any preexisting cracks, provided that there are preexisting cracks larger than a certain size [12]. For composites in which the fibers are held in place by frictional forces (e.g., the glass and glass ceramic composites mentioned above), this stress for matrix cracking, σ_o, is [10-13]

$$\sigma_o - \sigma_R = \left[\frac{6(1-\nu^2)\, K_o^2\, \tau\, f^2\, E_F\, E_c^2}{R\,(1-f)\, E_m^3}\right]^{1/3} , \qquad (1)$$

where σ_R is the axial residual stress in the matrix due to thermal contraction mismatch between the fibers and matrix, K_o is the fracture toughness of the unreinforced matrix, τ is the interface frictional stress, R is the fiber radius, f is the fiber volume fraction, ν is Poisson's ratio for the composite, and E_f, E_m E_c are the elastic moduli of the fibers, matrix and composite.

The insensitivity of σ_o to preexisting flaws has been confirmed experimentally in the SiC/glass ceramic composite by using a diamond indenter to introduce matrix cracks (larger than observable preexisting cracks) in a test specimen, and then observing the development of cracking during subsequent loading [8]. The first cracks to grow completely through the matrix in these tests invariably originated from locations other than the purposely induced damage. Because σ_o is independent of flaw size, there is nothing to be gained from searching for preexisting matrix flaws. However, NDE methods to measure nonuniformity of microstructural parameters such as f and τ would be useful in predicting premature matrix cracking.

The peak strength in tensile loading is dictated by fiber failure. After periodic matrix cracks form, the specimen can be viewed as a bundle of fibers that are connected by blocks of matrix. Failure of the bundle involves statistical fiber fracture, with stresses in the fibers being influenced by frictional forces due to the blocks of matrix. The bundle strength is dictated primarily by the average fiber strength, but is also influenced by the fiber/matrix properties and the shape parameter of the fiber strength distribution. It is noted that a statistical distribution of fiber strengths is required for the gradual decrease of load-carrying capacity beyond the peak load.

Low Strength Fibers. If the fiber strength is lower than a critical value, fiber failure accompanies the growth of a matrix crack. In this case, failure of the composite is catastrophic when the matrix crack extends through the specimen, and the composite appears "brittle". However, substantial toughening can still arise from the reinforcing fibers if the failure occurs behind the crack tip so that a zone of bridging fibers exists. The toughening effect is dependent upon the fiber strength, the interfacial properties and other microstructural parameters. The strength of the composite in this case is dependent upon preexisting cracks as well as the fracture toughness. Moreover, the preexisting cracks are characterized by both the total crack length and the size of the bridging zone.

Solutions have been obtained for a fracture mechanics model in which fibers are held in place by weak frictional forces and in which the fiber strengths are single-valued [13,16]. Weak frictional bonding is known to exist in the SiC and carbon fiber-reinforced glasses and glass ceramics, but in other systems the analysis may require further development. The single-valued fiber strength is a simplification that restricts the failure of bridging fibers to the region between the crack surfaces. A more realistic distribution of fiber strengths would allow fiber failure within the region embedded in the matrix, with continued crack-bridging effect as the fibers pull out of the matrix. In composites with random orientation of reinforcing fibers (or whiskers), strength distribution effects become less important, because bending stresses that develop in bridging fibers cause failure to occur in the region between the crack surfaces. The results of the analysis indicate that, in general, failure of the composite can involve several sequences of fiber failure or matrix cracking with increasing applied stress prior to catastrophic failure, depending on the initial crack configuration. However, the most impor-

tant ranges of behavior are represented by two initial configurations, the crack without an initial bridging zone (i.e., a notch cut by a saw) and the crack with a bridging zone extending over its entire length.

The applied stresses required to cause fiber failure or crack growth in the matrix for a fully bridged crack are shown in Fig. 2. The results are plotted in normalized form where $\sigma_n = 1.25\sigma_o$ and

$$c_n = (9\pi/4)\left[\frac{K_o R(1-f)E_c}{12\tau(1-\nu^2)f^2E_f}\right]^{2/3} \quad . \qquad (2)$$

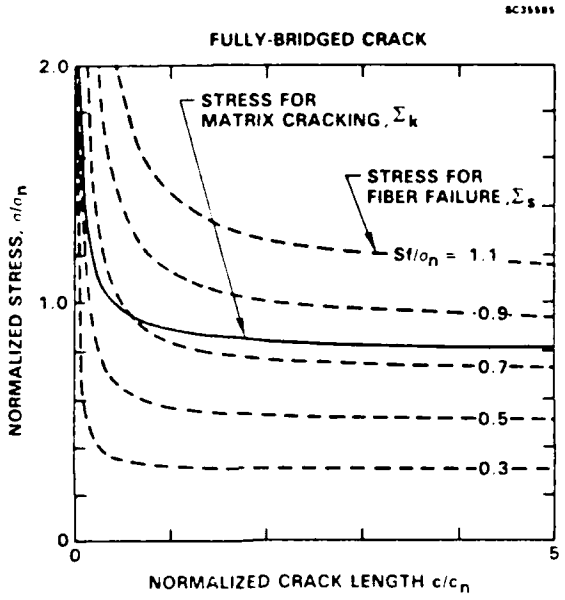

Fig. 2 Variation of stresses for matrix cracking and fiber failure with crack size for fully bridged crack.

For large cracks, both stresses approach steady-state values, 0.8 for matrix cracking and Sf/σ_n (where S is the absolute fiber strength) for fiber failure. The first event to occur upon loading depends on the initial crack length and fiber strength. If the crack is large and the fiber strength is $Sf/\sigma_n > 0.8$, then matrix cracking occurs first and further increase in applied stress is needed to cause fiber failure. This is the noncatastrophic mode of failure. But, if the fiber strength is < 0.8, catastrophic failure of the composite occurs when the applied stress equals the smaller of the matrix cracking or fiber failure stresses.

Failure from a crack that initially has no bridging fibers always begins with growth of the crack in the matrix. The stress required to cause continued crack growth is plotted as a function of the crack extension for various values of initial crack length, C_o, in Fig. 3. The matrix cracking stress in this case is an increasing function of crack extension, indicating that the growth is stable. This stable growth continues until a critical bridging zone develops (i.e., where fiber failure occurs), whereupon the composite fails catastrophically. The critical condition is indicated in Fig. 3 (broken curves) for several values of fiber strength. The analysis indicates that the applied stress and crack size at the critical condition are related by [16]

$$\sigma = K_c/(\pi c)^{1/2} \tag{3}$$

where

$$K_c = K_o \left[\left(\frac{E_c}{E_m}\right)^2 + \left(\frac{S^3 R}{4\tau K_o^2 (1-\nu^2)}\right)\left(\frac{f(1-f)E_m}{E_f}\right)\right]^{1/2} . \tag{4}$$

In this case, NDE to detect preexisting cracks would clearly be beneficial for reliability prediction.

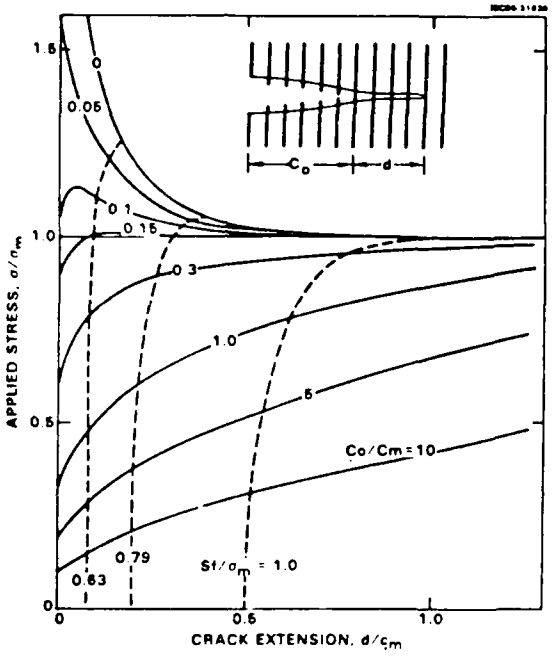

Fig. 3 Variation of stress required to extend a partly bridged crack (solid curves, for various initial unbridged crack sizes) with crack extension. Broken curves represent loci of the condition for catastrophic failure for various fiber strengths.

Transitions in Failure Mechanism. The results in Fig. 3 indicate that the transition from catastrophic to noncatastrophic failure for initially fully bridged cracks occurs at $Sf/\sigma_n = 0.8$. The parameter Sf/σ_n is dependent upon the microstructural properties of the composite [16]:

$$Sf/\sigma_n = \left[\frac{S^3 R\, f(1-f)\, E_m^3}{12\tau\, K_o^2 (1-\nu^2)\, E_f E_c^2}\right]^{1/3} . \tag{5}$$

More generally, the transition value of Sf/σ_n is also dependent upon the initial size of the bridging zone associated with the dominant crack, as shown in Fig. 4. For composites in which the parameter Sf/σ_n is larger than the value indicated by the curve labeled S_4, failure is always noncatastrophic. For Sf/σ_n smaller than values defined by curve S_3, failure is always catastrophic. And for values in the small region between the two curves, either failure mechanism can occur, depending on the initial total crack length.

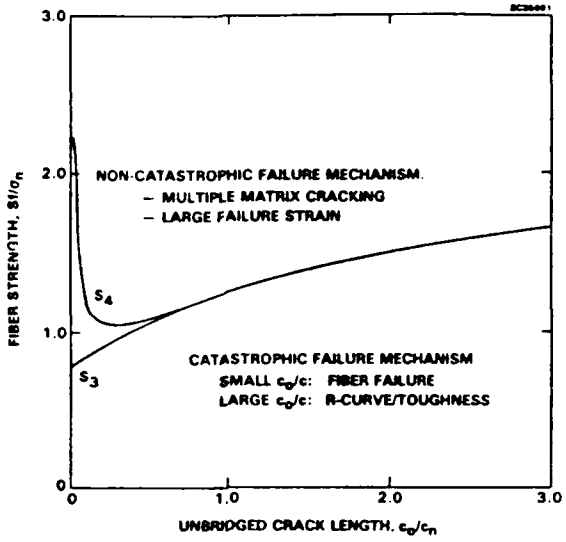

Fig. 4 Condition for transition between catastrophic and non-catastrophic failure mechanisms.

2.2 Flexural Loading

A beam loaded in flexure experiences tensile and compressive stresses of equal magnitude at the surfaces, and shear on the mid plane of the beam, between the loading lines. The ratio of the magnitudes of the maximum tensile and shear stresses is proportional to the ratio of the separation of the loading lines to the specimen thickness. Consequently, the failure mechanism is also dependent upon these dimensions.

For long thin beams, failure begins with matrix cracking, as in tensile loading, but the matrix cracks arrest as they approach the mid plane of the beam. Subsequently, failure of the beam occurs by compressive damage [8] (fiber buckling and matrix crushing). Once matrix cracking occurs, the composite becomes more compliant on the tensile side of the beam than on the compressive side, so that the neutral axis shifts toward the compressive surface, and the magnitude of the stress at the compressive surface becomes larger than that at the tensile surface. Thus, even though the strength of the composite is higher in uniaxial compressive loading than in uniaxial tensile loading, the load redistribution in the beam causes failure in compression [8]. Relations between compressive failure stress and microstructure are not well defined, but the fiber buckling stress would be expected to be influenced by nonuniformity in the fiber distribution, as well as fiber straightness and alignment.

For short thick beams, failure ocurs in shear between the inner and outer loading points. This involves matrix microcracking, which is apparently influenced by shear stress concentrations in the matrix between bundles of fibers that are nonuniformly distributed [21].

3. LAMINATED COMPOSITES

Laminated composites have tensile properties intermediate between the axial and transverse properties of uniaxially reinforced composites, as shown in Fig. 5 for the SiC/glass-ceramic composite [9]. However, failure processes are influenced by interaction of the laminates, especially from the interlaminar residual stresses. Three main stages of

damage formation have been identified, at stresses σ_d, σ_c and σ [9]. Initial deviation from linearity at stress σ_d is associated with formation of delamination cracks at the edge of the specimen. These cracks lie parallel to the applied stress and within the transverse layer adjacent to the laminate interface. The cracks are driven by edge stresses arising from both residual interlaminar stresses and elastic anisotropy. Detailed fracture analysis of crack initiation is not available. The second mode of damage involves periodic matrix cracking normal to the applied load at stress σ_c. In the SiC glass ceramic composite, the cracks developed in both the axial and transverse laminates at about the same load. The formation of the cracks can be analyzed in terms of the results of Sect. 2, with the additional influence of interlaminar residual stresses [9]. The peak stress is determined by fiber failure, which leads to large openings of matrix cracks and formation of large delamination cracks.

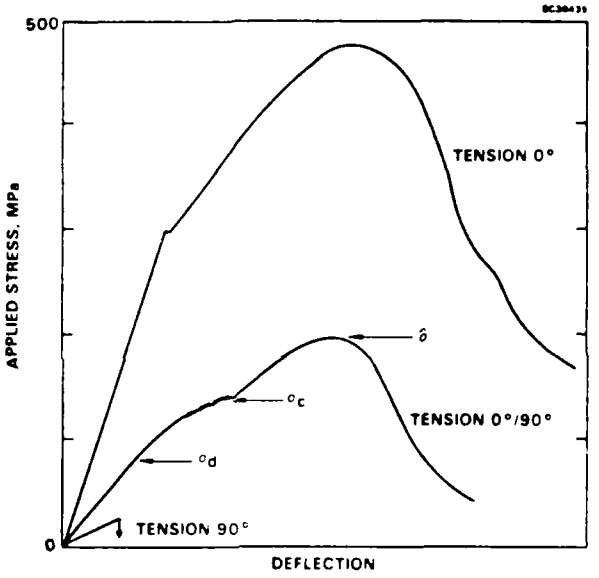

Fig. 5 Comparison of load-deflection curves for unidirectional and cross-ply laminated composites of SiC/glass ceramic.

4. OPPORTUNITIES FOR NDE

The results described in Sects. 2 and 3 indicate that the mechanical behavior of composites and the role of defects can be very sensitive to microstructural properties and the applied stress state. Nevertheless, a number of examples have been defined where NDE could play an important role in assessing reliability. These involve not only detection of flaws, but also evaluation of microstructural characteristics, such as interfacial properties, residual stresses, and uniformity of the fiber distribution.

The nature of the fiber/matrix interface is the key microstructural property that is subject to processing variability. In frictionally bonded composites, the magnitude of the stress that resists sliding at the interface determines the matrix cracking stress and the fracture toughness in the noncatastrophic and brittle modes of failure (Eqs. (1) and (4)), as well as dictating which of the failure mechanisms occurs (Eq. (5)). Therefore, nondestructive methods for measuring τ (e.g., based on internal friction measurements) would be beneficial.

Residual stresses arise from different thermal contractions of fibers and matrix and, in laminated composites, from anisotropy in contraction of individual layers giving rise to interlaminar stresses. These stresses have a direct influence on the stress for matrix cracking (Eq. (1)) and on delamination in cross-plied composites [9]. Moreover, the residual stress normal to the fiber/matrix interface influences the sliding resistance. Residual stresses could be evaluated using x-ray or acoustic methods.

Nonuniformities in fiber distribution in a composite influence the transition between catastrophic and noncatastrophic failure in both tension and flexure. In particular, a region of missing fibers would allow matrix cracking at reduced applied stress (Eq. (1)). Although the crack may arrest at an area of higher fiber concentration, the crack so formed has a large unbridged area, which may allow brittle failure in a composite that would otherwise (i.e., for fully bridged cracks) fall within the region of noncatastrophic failure in Fig. 4. In flexural loading, nonuniform fiber distributions have the additional influence of creating stress concentrations that tend to induce shear failure. Therefore, methods for detecting nonuniformity of fiber distribution would be useful for quality control.

There are several areas where detection of cracks would be useful to predict reliability. The most obvious is in tensile loading of composites that fail catastrophically. The strength in this case is very sensitive to the preexisting cracks which may be partly bridged by fibers or whiskers. For cracks with bridging zones that are sufficiently small for the R-curve behavior depicted in Fig. 3 to apply, the strength can be related directly to the unbridged crack size. This is expected to be the case for many whisker-reinforced composites. The size of the unbridged area is also critical for determining the failure mechanism (Fig. 4). However, in general, both the total crack size and the size of the bridging zone must be evaluated. This problem is related to previous studies of acoustic scattering from cracks in Si_3N_4 [3,4], in which a strong influence of bridging from asperities on the crack surface was found for unloaded cracks.

In composites that fail noncatastrophically, neither the ultimate strength nor the matrix cracking stress are influenced by preexisting cracks. However, the formation of matrix cracks degrades the elastic properties of the composite and leaves the internal fibers accessible to environmental corrosion and fatigue damage. Therefore, detection of matrix cracking would be important for in-service reliability or lifetime monitoring. Similar comments apply to laminated composites in which failure is preceded by both delamination and matrix cracking.

ACKNOWLEDGEMENT

Funding for this work was supplied by the U.S. Office of Naval Research, Contract No. N00014-85-C-0416.

REFERENCES

1. A.G. Evans, "Structural Reliability: A Processing-Dependent Phenomenon," J. Am. Cera . Soc. 65 (3), 127-37 (1982).
2. B.T. Khuri Yakub, G.S. Kino and A.G. Evans, "Acoustic Surface Wave Measurement of Surface Cracks in Ceramics," J. Am. Ceram. Soc. 63 (1-2), 65-71 (1980).

3. D.B. Marshall, A.G. Evans, B.T. Khuri-Yakub, J.W. Tien and G.S. Kino, "The Nature of Machining Damage in Ceramics," Proc. Roy. Soc. A385, 461-75 (1983).
4. J. Tien, B.T. Khuri-Yakub, G. Kino, A.G. Evans and D.B. Marshall, "Surface Acoustic Wave Measurements of Surface Cracks in Ceramics," J. NDE 2 (3-4), 219-29 (1981).
5. L.R. Clark, C.H. Chou, B.T. Khuri Yakub and D.B. Marshall, "Ultrasonic Characterization of Machining Damage in Ceramics," in Rev. of Prog. in Quantitative NDE, eds., D.O. Thompson and D.E. Chimenti, Plenum, 1985.
6. B.R. Lawn, this volume.
7. D.B. Marshall, "Strength Characteristics of Transformation-Toughened Ceramics," J. Am. Ceram. Soc. 69 (3), 173-80 (1986).
8. D.B. Marshall and A.G. Evans, "Failure Mechanisms in Ceramic-Fiber/Ceramic-Matrix Composites," J. Amer. Ceram. Soc. 68 (5), 225-31 (1985).
9. O. Sbaizero and A.G. Evans, "Tensile and Shear Properties of Laminated Ceramic Matrix Composites," J. Amer. Ceram. Soc. 69 (6), 481-86 (1986).
10. J. Aveston, G.A. Cooper and A. Kelly, "Single and Multiple Fracture," pp. 15-26 in the Properties of Fiber Composites, Conf. Proc. Nat. Physical Lab., IPC Science and Technology Pres. Ltd., Surrey, England, 1971.
11. J. Aveston and A. Kelly, "Theory of Multiple Fracture of Fibrous Composites," J. Mat. Sci. 8, 352-62 (1973).
12. D.B. Marshall, B.N. Cox and A.G. Evans, "The Mechanics of Matrix Cracking in Brittle-Matrix Fiber Composites," Acta. Met. 33 (11), 2013-21 (1985).
13. D.B. Marshall and A.G. Evans, "Tensile Strength of Ceramic Fiber Composites," in Fracture Mechanics of Ceramics, eds., R.C. Bradt, D.P.H. Hasselman, A.G. Evans and F.F. Lange, Plenum 7, 1-15 (1986).
14. B. Budiansky, J.W. Hutchinson and A.G. Evans, "Matrix Fracture in Fiber-Reinforced Ceramics," J. Mech. Phys. Solids 34 (2), 167 (1986).
15. B. Budiansky, "Micromechanics II," in Proc.of 10th U.S. Nat. Cong. of Applied Mechanics, 1986.
16. D.B. Marshall and B.N. Cox, "Tensile Strength of Brittle Matrix Composites: Influence of Fiber Strength," submitted to Acta. Met.
17. J.J. Brennan and K.M Prewo, "Silicon Carbide Fiber-Reinforced Glass-Ceramic Matrix Composites Exhibiting High Strength and Toughness," J. Mat. Sci. 17 (8), 2371-83 (1982).
18. K.M. Prewo, "A Compliant, High Failure Strain, Fiber-Reinforced Glass Matrix Composite," J. Mat. Sci. 17 (12), 3549-63 (1982).
19. R.A.J. Sambell, A. Biggs, D.C. Phillips and D.H. Bowen, "Carbon Fiber Composites with Ceramic and Glass Matrices, Part 2 - Continuous Fibers," J. Mat. Sci. 7 (6), 676-81 (1972).
20. D.C. Phillips, "Interfacial Bonding and the Toughness of Carbon Fiber-Reinforced Glass and Glass Ceramics," J. Mat. Sci. 9 (11), 1847-54 (1974).
21. A.G. Evans, M.D. Thouless, D.P. Johnson-Walls, E.Y. Luh and D.B. Marshall, "Some Structural Properties of Ceramic Matrix Fiber Composites," 5th Int. Conf. on Composite Materials, eds., W.C. Harrigan, J. Strife and A.K. Dhingra, Metallurgical Society, PA (1985).
22. G.A. Cooper and J.M. Silwood, "Multiple Fracture in a Steel-Reinforced Epoxy Resin Composite," J. Mat. Sci. 7, 325-33 (1972).

5.0 STRENGTH AND INTERFACIAL PROPERTIES OF CERAMIC COMPOSITES

Proceedings of MRS Symposium, "Advanced Structural Ceramics", in press.

STRENGTH AND INTERFACIAL PROPERTIES OF CERAMIC COMPOSITES

D.B. MARSHALL
Rockwell International Science Center, 1049 Camino Dos Rios, Thousand Oaks, CA 91360

ABSTRACT

Results of recent micromechanics analyses of the reinforcing influence of frictionally bonded fibers in ceramic composites are summarized. Direct measurements of the fiber/matrix interface properties are also discussed.

INTRODUCTION

Tensile strength and toughness of materials that are inherently brittle can be dramatically improved by fiber reinforcement. Generally, this requires a relatively low-toughness interface between the fibers and matrix to permit debonding and sliding, and thereby allow fibers to bridge the crack surfaces. Fracture mechanics models have been developed recently to evaluate the influence of such bridging zones on the mechanisms of crack growth. Solutions have been obtained for composites in which there is no bonding at the interface, but sliding is resisted by friction. Novel methods have also been devised for measuring the mechanical properties of interfaces directly at individual fibers in weakly bonded composites. Some results from the fracture mechanics analysis and interface measurements are briefly summarized below. More complete descriptions are contained in Refs. [1-6].

FRACTURE MECHANICS MODELING

Fibers that bridge a crack cause a reduction of crack opening, and thereby reduce the stress at the crack tip. The reduction of stress can be evaluated by replacing the section of fiber between the crack surfaces by closure tractions equal to the stress in the fiber and using a Green's function [7] to calculate the stress intensity factor. The calculation also requires evaluation of the crack opening displacements at every location in the crack, for the stress in each fiber is related, via the mechanics of the frictional sliding, to the crack opening. The displacements were obtained by numerical solution of an integral equation derived by Sneddon [8].

In general, failure from a preexisting crack with a zone of bridging fibers may occur by one of several sequences of events. Failure may initiate either by growth of the crack in the matrix or by failure of the bridging fibers. Subsequently, each of these fracture processes can occur either unstably or stably, leading to failure of the composite at constant load or requiring further load increase to cause failure. The sequence leading to failure must be evaluated in order to calculate the strength or toughness of the composite. This entails calculation of the applied stresses needed to cause both matrix crack growth and failure of the last fiber in the bridging zone (i.e., the most highly stressed fiber) as a function of both the total crack size and the length of the bridging zone.

The results of such calculations for two extreme initial crack configurations are summarized in Figs. 1 and 2. In Fig. 1, the applied stresses necessary to cause matrix cracking and fiber failure, for an initially fully bridged crack, are plotted in normalized form (see Refs. [1

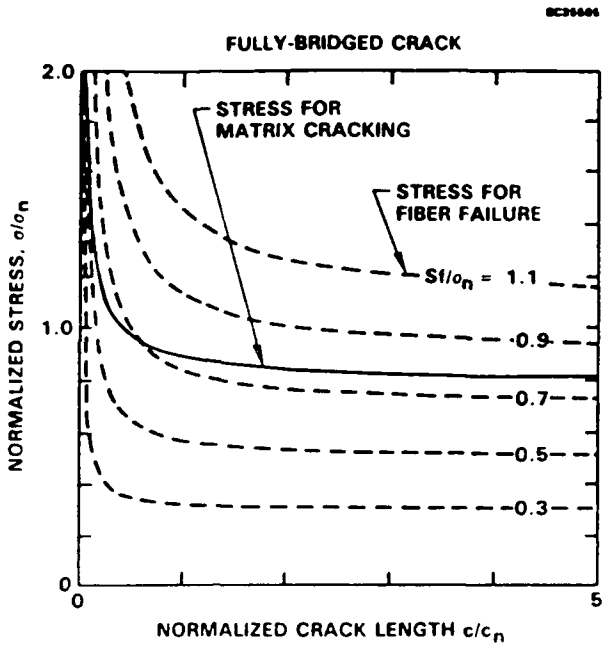

Fig. 1 Applied stresses required to extend a fully bridged crack in the matrix and to fracture bridging fibers (after Ref. [1]).

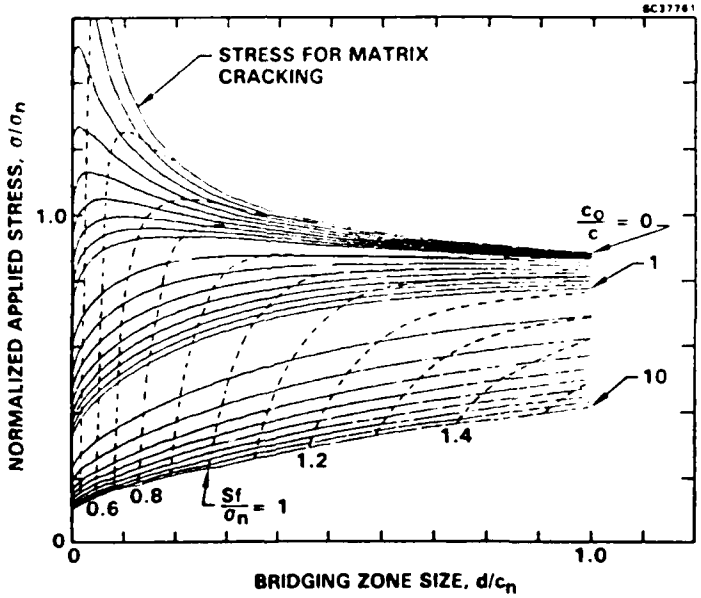

Fig. 2 Applied stress needed to extend an initially unbridged crack in the matrix, plotted as a function of crack extension, d, for various initial crack lengths, c_0. Broken curves represent the condition at which catastrophic failure occurs, i.e., the bridging fibers fracture (after Ref. [1]).

and 3]) for various values of normalized fiber strength. For high-strength fibers ($Sf/\sigma_n > 0.8$, where S is the fiber strength, f the volume fraction of fibers, and σ_n a normalizing stress (see Eq. (1)), the stress for matrix cracking is lower than the stress for fiber failure, so that the crack grows in the matrix first. Moreover, the crack can extend indefinitely

without causing fiber fracture, and an increased applied stress is needed to cause failure of the composite. This leads to a noncatastrophic mode of failure involving multiple matrix cracking. This mechanism has been observed in glasses and glass-ceramics that are reinforced by carbon and SiC fibers [9-12]. The steady-state matrix cracking stress in Fig. 1 is the well-known solution of Aveston, Cooper and Kelly [9]:

$$\sigma_o = 0.8\ \sigma_n = \left[\frac{6(1-\nu^2)K_o^2\tau f^2 E_f E_c}{R(1-f)E_m^3}\right]^{1/3} , \qquad (1)$$

where K_o is the toughness of the unreinforced matrix, τ is the frictional stress at the fiber/matrix interface, R is the fiber radius, ν is the Poisson's ratio of the composite, and E_f, E_m and E_c are the elastic moduli of the fibers, matrix and composite. For lower fiber strengths ($Sf/\sigma_n < 0.8$), fiber failure occurs before matrix cracking, and is followed by unstable matrix crack growth. Therefore, in this case, the composite strength is determined by the stress for fiber failure.

A crack that initially has no bridging zone always grows stably in the matrix with increasing applied stress. This stress is plotted as a function of crack extension for various initial crack lengths, c_o, in Fig. 2. Stable growth continues until the stress in the bridging fibers builds up to the critical value needed to break the fiber, whereupon the composite fails catastrophically. This critical condition, for various normalized fiber strengths, is indicated by the broken lines in Fig. 2. At the critical condition, the bridging effect of the fibers is equivalent to an increase in the fracture toughness given by

$$K_p/K_c = \left[1 + 4(Sf/\sigma_n)^3\right]^{1/2} - 1 , \qquad (2)$$

where

$$(Sf/\sigma_n)^3 = \left(\frac{S^3 R}{12\tau K_o^2}\right)\left(\frac{f(1-f)E_m^3}{(1-\nu^2)E_f E_c^2}\right) . \qquad (3)$$

PROPERTIES OF THE INTERFACE

It is clear from Eqs. (1) and (3) that the magnitude of the interfacial frictional stress plays a key role in determining the strengthening and toughening, as well as the failure mechanism of the composite. A method for measuring the frictional stress at individual fibers is illustrated schematically in Fig. 3. The technique involves pushing the end of a fiber with a sharp indenter and measuring the resultant displacement of the fiber beneath the surface of the matrix. Analysis of the mechanics of fiber sliding under this condition allows the frictional stress to be obtained from measurements of the force applied to the fiber and the displacement.

A standard Vickers hardness testing instrument can be used to obtain force and displacement measurements at the peak load condition [4], thereby providing an average value of the frictional stress over the area of interface that undergoes sliding. However, more information can be obtained using an instrument that allows continuous measurement of force and displacement during loading (and unloading) [6]. Results obtained from a SiC/

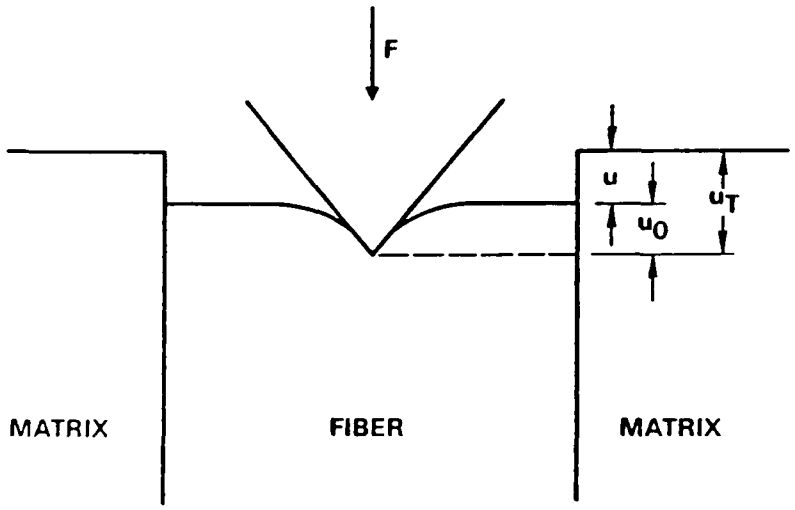

Fig. 3 Schematic diagram of indentation experiment to measure interfacial sliding resistance (after Ref. [6]).

glass-ceramic composite* using a nano indenter instrument** are shown in Fig. 4. The curves represent predictions of the force-displacement relation for purely frictional sliding with constant frictional stress during loading, unloading, and reloading. The data follow the prediction very closely during initial loading, indicating that the frictional stress is uniform along the interface (each force increment causes the area of interface over which fiber/matrix sliding occurs to increase). However, during unloading and subsequent reloading, when reverse sliding occurs, the results indicate that the frictional stress decreases.

The results in Fig. 4 also indicate that sliding at the interface in this composite does not require prior debonding. Analysis of combined debonding and frictional sliding during the initial loading indicates that the force-displacement relation becomes [6]

$$u = F^2/4\pi^2R^3\tau E_f - 2\Gamma/\tau \quad , \tag{4}$$

where Γ is the fracture surface energy associated with mode II debonding. Fitting Eq. (4) to the data in Fig. 4 gives $\tau = 2.9$ MPa and $\Gamma \leq 0.4$ J/m^2. This upper bound for the value of Γ, obtained by taking into account maximum measurement errors for the data in Fig. 4, is in the range of energies associated with Van der Waals bonds.

ACKNOWLEDGEMENTS

The research summarized here was done in collaboration with B.N. Cox, Rockwell International Science Center, W.C. Oliver, Oak Ridge National Laboratory, and A.G. Evans, University of California at Santa Barbara. Funding was provided by the U.S. Office of Naval Research, Contract No. N00014-85-C-0416.

* United Technologies Research Center, East Hartford, CT
** Microscience Inc., Braintree, MA

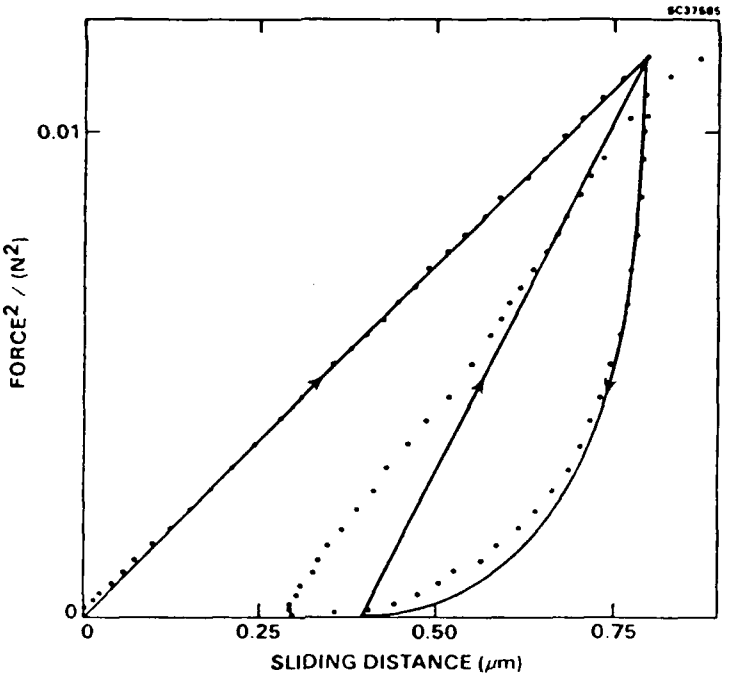

Fig. 4 Forces and displacements measured during indentation (loading, unloading, reloading) of fiber as in Fig. 3. Solid curves are theoretical predictions for sliding opposed by constant frictional stress (after Ref. [6]).

REFERENCES

1. D.B. Marshall and B.N. Cox, "Tensile Properties of Brittle Matrix Composites: Influence of Fiber Strength," to be published in Acta Met.
2. D.B. Marshall, B.N. Cox and A.G. Evans, Acta Met. 33 (11), 2013-21 (1985).
3. D.B. Marshall and A.G. Evans, in Fracture Mechanics of Ceramics 7, Ed., R.C. Bradt, A.G. Evans, D.P.H. Hasselman and F.F. Lange (Plenum), 1986, pp. 1-15.
4. D.B. Marshall, J. Am. Ceram. Soc. 67 (12), C259-60 (1984).
5. D.B. Marshall, in Ceramic Microstructures '86: Role of Interfaces, eds., J.A. Pask and A.G. Evans (Plenum, in press).
6. D.B. Marshall and W.C. Oliver, J. Am. Ceram. Soc., in press.
7. G.C. Sih, Handbook of Stress Intensity Factors, Lehigh University Press, Bethlehem, PA (1973).
8. I.N. Sneddon and M. Lowengrub, Crack Problems in the Classical Theory of Elasticity, Wiley, NY (1969).
9. J. Aveston, G.A. Cooper and A. Kelley, in Properties of Fiber Composites, Conf. Proc. Nat. Physical Lab. IPC Science and Technology Pres. Ltd., Surrey, England, 1971, pp. 15-26.
10. D.B. Marshall and A.G. Evans, J. Am. Ceram. Soc. 68 (5), 225-31 (1985).
11. J.J. Brennan and K.M. Prewo, J. Mater. Sci. 17 (8), 2371-83 (1982).
12. R.A.J. Sambell, A. Briggs, D.C. Phillips and D.H. Bowen, J. Mater. Sci. 7 (6), 676-81 (1972).

END

12-87

DTIC